I&EC research
Industrial & Engineering Chemistry Research

Review

Cite This: Ind. Eng. Chem. Res. 2018, 57, 4479−4504

pubs.acs.org/IECR

Thermoplastic-Toughened High-Temperature Cyanate Esters and Their Application in Advanced Composites

Ahmed Inamdar,[†] Jayalakshmi Cherukattu,[‡] Anoop Anand,[‡] and Balasubramanian Kandasubramanian*[,†]

[†]Department of Materials Engineering, Defence Institute of Advanced Technology (DU), Ministry of Defence, Girinagar, Pune-411025, India

[‡]Composites Research Centre, Research and Development Establishment (Engineers), DRDO, Ministry of Defence, Pune-411015, India

ABSTRACT: Cyanate esters (CEs) are recognized as matrix materials in composites for high-temperature structural applications, owing to their excellent thermal and dimensional stability, resistance to micro-cracks, low moisture absorption, and low dielectric loss. Though the brittle nature of CEs curtails their effective utilization, thermoplastic toughening has paved the way to circumvent their innate brittle attribute by virtue of the resulting two-phase morphology. This Review enumerates detailed deliberation on thermoplastic toughening of CEs and their semi-interpenetrating networks. Further, the effects of various decisive variables like thermoplastic concentration, molecular weight, and curing conditions are also reviewed and disserted in detail. In addition, the mechanical properties of numerous developed CE blends and their toughening mechanism are deliberated to elucidate their substantial engineering applications. This Review renders a detailed contemplation on thermoplastic toughening of CEs, composite fabrication methodology, and their structural integrity for high-temperature applications.

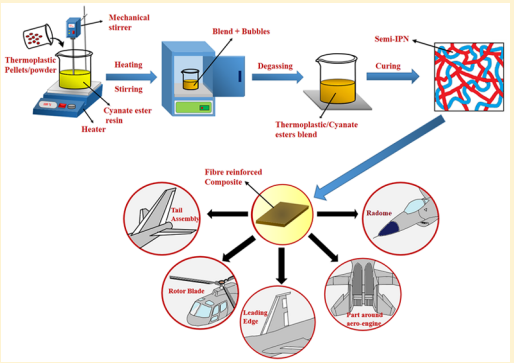

1. INTRODUCTION

Reduction in the weight of a component, especially in space applications, is coupled with improvements in the performance of the system along with fuel economy and increase in payload capacity. The development of composite materials has provided designers the flexibility to tailor properties such as strength, modulus, fracture toughness, and thermal stability. A recent up-and-coming trend in the composites industry is to develop composites for high-temperature structural applications, such as parts around aero-engines, leading edges, rotor blades, etc. In the past, epoxy-based composites with high-strength fibers like carbon/glass have been the major class of material catering to the needs of such specialty applications.[1,2] However, current epoxy-based systems have drawbacks of excessive water absorption and residual stresses, leading to micro-cracks when thermally cycled.[3] Also, the maximum service temperature of these epoxy systems for structural application is approximately 177 °C, while further introduction of wet environments restricts this to 149 °C.[4] Hence, researchers are searching for matrix materials exhibiting high service temperature along with improved toughness and reduced water uptake. Cyanate esters, bismaleimides, and polyimides are a few of the choices of materials that are being continuously evaluated for their capability to match the requirements for specialty applications.[4−12]

Cyanate esters (CEs) are becoming a popular choice in high-temperature specialty applications because of their excellent mechanical and physical properties, including high glass transition temperature (T_g), excellent thermal stability, low dielectric loss, low moisture uptake, and low flammability.[4] Compared with epoxies and bismaleimides (BMIs), CEs are inherently more hydrophobic, and cured neat resins absorb only 0.5−2.5 wt% of water.[4,13] The cost of CEs is also comparable with that of high-performance epoxies and less than that of BMIs. Along with high-temperature structural space applications, CEs have tremendous potential in the electronics industry for making printed circuit boards, building radome structures, etc.[4,14−16]

Monomers of CEs polymerize by a cyclotrimerization reaction to yield a cyanurate-linked polymer network also referred to as a triazine ring. CEs are available in a variety of forms including liquid, solid, semisolid, and solution and have excellent shelf-life at room temperature.[4] High cross-link density associated with CEs contributes to achieving a high T_g but, on the flip side, can be blamed for the low fracture toughness. Therefore, enhancing the toughness of CE resins is a major concern in order to use them as matrix in high-performance applications. Various approaches have been studied to enhance the toughness of CEs, including blending with epoxies, BMIs, reactive rubbers, and engineering thermoplastics.[17−27] Thermoplastics toughening is attractive and

Received: December 19, 2017
Revised: February 24, 2018
Accepted: March 7, 2018
Published: March 7, 2018

DOI: 10.1021/acs.iecr.7b05202
Ind. Eng. Chem. Res. 2018, 57, 4479−4504

effective toughening mechanism, as the resulting blend system retains important inherent properties of CEs. Engineering thermoplastics like poly(ether imide), polysulfones, polyimide, poly(ether sulfone), polyacrylate, etc. are miscible in cyanate monomers, forming homogeneous blends.[27−32] Handling and processing of these blends are similar to those for epoxies; hence, well-developed processing techniques known for epoxies can easily be imported. Curing of these blends leads to phase separation, forming semi-interpenetrating networks with properties greatly depending upon the morphology obtained.[28−30] Various morphologies are observed, including phase-inverted and co-continuous. Hence, understanding the effects of morphology-controlling variables like molecular weight, curing conditions, and blend composition is crucial in order to tailor the final properties of blends.

CEs are extensively modified and evaluated to enhance their toughening characteristics using various approaches such as incorporating fillers, blending with elastomers or thermoplastics, using high-temperature thermosets, etc. Despite the advantages of thermoplastic toughening in high-temperature thermosets, it has not been extensively reported and reviewed. Hence, in this Review, a comprehensive study on the thermoplastic toughening of CEs and tailoring of the final properties of the blend through control of morphology is presented. In this abstraction, various toughening mechanisms involved in modification of high-temperature thermosets, their processing routes, and control of variables involved in the processing are reviewed in detail. Further, we delineate various thermoplastics for their toughening potential in CEs in addition to the number of different morphology-dominating variables and mechanical properties of blends. Subsequently, we demonstrate the utilization of these toughened blends in the development of high-temperature composites for engineering applications like radomes, tail assembly, leading edges, rotor blades etc. Though it is ambitious to cover the entirety of the published work on this topic, we have made an attempt to compile most of the literature which can make the greatest potential impact in this field.

2. CONCEPT OF POLYMER BLENDS AND INTER-PENETRATING NETWORKS

Polymer blends are defined as "a mixture of at least two polymers or copolymers with their concentration above 2 wt %",[33] and a new class of materials has improved properties, comprising the advantages of each polymer constituent. Blending is an easy and economical method for developing new polymeric material, allowing tailoring of properties in accordance with end use by appropriate selection of the polymer combinations. Polymer blends are broadly classified into two major types: miscible blends and immiscible blends.

Miscible blends are homogeneous single-phase systems that can undergo phase separation while curing and generates different morphologies. Since the properties of a cured polymer blend depend on the final morphology obtained, various researchers have undertaken extensive studies on the miscibility and phase separation behavior of polymer blends.[4,34−36]

2.1. Miscible and Immiscible Blends. Thermodynamically, blends are classified into miscible, partially miscible, or immiscible on the basis of the Gibbs free energy (ΔG_{mix}) value of the mixture,[33,37] given by the following equation:

$$\Delta G_{mix} = \Delta H_{mix} - T\Delta S_{mix} \quad (1)$$

In order to get a miscible solution (binary blend), the following two conditions need to be satisfied:

First,

$$\Delta G_{mix} < 0 \quad (2)$$

Second,

$$\left(\frac{\partial^2(\Delta G_{mix})}{\partial \phi_i^2}\right)_{T,P} > 0 \quad (3)$$

where ΔG_{mix} is the Gibbs energy of mixing and ϕ is the composition, usually taken as the volume fraction of one of the components.

Here, ΔS_{mix} is the entropy of mixing. It is always positive and, therefore, favorable for mixing. ΔH_{mix} is the enthalpy change due to mixing, which can be either endothermic or exothermic. Exothermic reactions that occur during mixing, which drive the system toward miscibility, are possible only if strong specific interactions like polymer hydrogen bonding, dipole−dipole, and ionic interactions are present in polymer components.[38] These specific interactions can be understood using techniques such as Fourier transform infrared (FTIR) spectroscopy, small-angle neutron scattering (SANS), and nuclear magnetic resonance (NMR) spectroscopy. It is believed that blends which show a single T_g are miscible blends. However, T_g is insensitive to thermodynamic miscibility and depends on the degree of dispersion. Hence, a single T_g does not necessarily represent miscible blends, as immiscible blends with fine dispersions of phases have also shown single T_g values.[33] Zhan et al.[39] reported that a blend of CE/poly(ether imide) (PEI) shows a single T_g at an early stage of curing (up to 6 min for curing at 150 °C) and then two T_g peaks for each component. Their study concluded that the CE/PEI blend was homogeneous up to 6 min at 150 °C curing and then phase-separated.

The most popular theory for defining thermodynamic miscibility of polymer blends was developed by Flory and Huggins in 1941.[33] This theory defines miscibility and helps us to construct a phase diagram of blends. According to this theory, free energy of mixing is given by

$$\Delta G_{mix} = RTV\left[\left(\frac{\phi_1}{V_1}\right)\ln(\phi_1) + \left(\frac{\phi_2}{V_2}\right)\ln(\phi_2)\right] + B\phi_1\phi_2 \quad (4)$$

where $\chi'_{12} = \chi_{12}/V_1$ and $B = \chi_{12}RT(V/V_1)$, with V_i molar volume, ϕ_i volume fraction, and χ_{12} a binary interaction parameter.

Flory and Huggins defined the critical binary interaction parameter ($\chi_{12\ crc}$), and blends with binary interaction parameter above the critical point result in phase separation. Zhan et al.[31,39] applied the Flory−Huggins equation to draw a phase diagram for CE/PEI and concluded that 15 parts per hundred (phr) concentration was a critical point corresponding to the lowest curing conversion of CE. Further, Zhan reported that, for the phase separation mechanism at a concentration of thermoplastic lower than the critical point in conversion versus composition transformation diagram results in a nucleation and growth (NG) mechanism, while for higher concentration above the critical point it leads to phase separation by spinodal decomposition (SD).[39] Borrojio et al.[40] and Pascault et al.[25] investigated rubber-toughened CE blends using the Flory−Huggins equation and concluded that phase separation occurs due to changes in free energy dominated by changes in entropy

DOI: 10.1021/acs.iecr.7b05202
Ind. Eng. Chem. Res. 2018, 57, 4479−4504

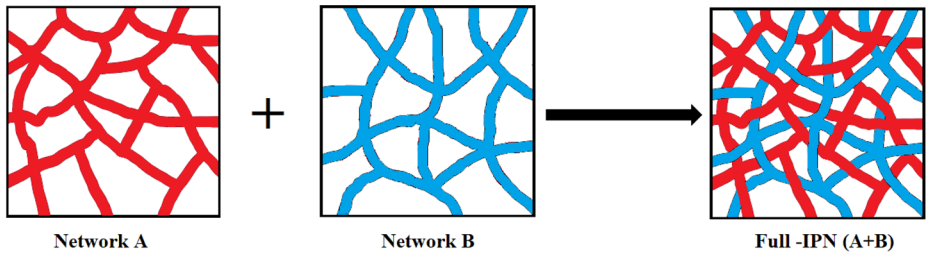

Figure 1. Schematic of a full-interpenetrating network.

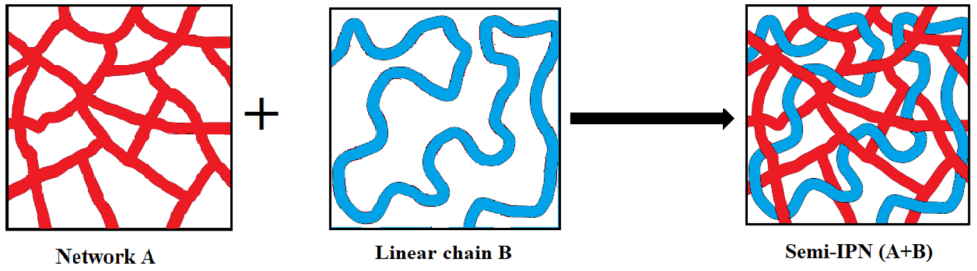

Figure 2. Schematic of a semi-interpenetrating network.

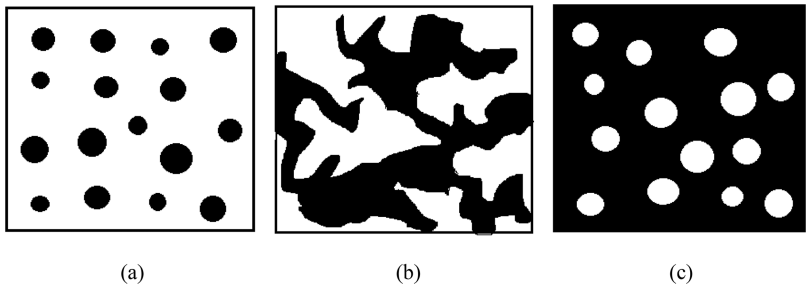

Figure 3. Schematic of phase separation and morphology changes with increasing thermoplastic concentration: (a) particulate, (b) co-continuous, and (c) phase-inverted.

during polymerization. The solubility parameter approach is also used to define soluble blend combinations. The solubility parameter of CE is $\delta = 25.23\ (\mathrm{J/mL})^{1/2}$, and polymers having solubility parameter values close to the CE solubility parameter are defined as miscible in CEs.[33,41]

2.2. Interpenetrating Networks (IPNs). IPNs form an another class of polymeric component system, having two cross-linked polymer networks without any covalent bonding in between them. Figure 1 shows a schematic representation two cross-linked networks, A and B, combining to form an interlinked full-IPN. Another binary network with only one polymer cross-linked is also referred to as an IPN but, more precisely, a semi-IPN. As shown in Figure 2, linear chain B combines with network A to lead to a semi-IPN in which only one polymer is in network form.

IPNs can be prepared by mixing two monomers and then cross-linking them to form a network or by dissolving the second polymer in the network of the first polymer followed by curing the second polymer to form a network. Another route leading to IPNs is the blending of two polymers which are thermodynamically miscible and then cross-linking them to form a network. IPNs may undergo phase separation following kinematics like NG and SD and follow four distinct stages to yield the final morphology.[42]

During the first stage, both polymers remains soluble and form a clear transparent solution. As polymerization proceeds to stage two, the solution clouds up and phase separation occurs following a NG mechanism. In stage three, an interconnected cylinder develops following a SD mechanism. Further, as the polymerization proceeds to the stage four, it results in growth of domains.[34,43] This dual phase continuity causes an increase in the area under the loss modulus vs temperature curve near the T_g.[44] A morphology with smaller domain sizes shows one broad glass transition peak, while with larger domain sizes two distinct glass transitions are observed.[28,45] IPNs are considerably more important, as they combine two non-compatible polymers in network form, like brittle high-temperature thermosets and tough thermoplastics. The resulting material combines the inherent advantages of the individual components, such as the toughness and ease of processing of thermoplastics and high service temperature of thermosets.

3. MORPHOLOGY AND PHASE SEPARATION

Phase separation occurring in soluble blends of amorphous thermoplastics/thermosets is an effective means for toughening the thermoset without degrading its inherent properties.[33] Co-continuous and phase-inverted morphologies are known to improve mechanical properties for this type of system.

Figure 3 shows the morphology change as a function of concentration of added component. Component A, which is represented in black, is added in component B, shown in white. At lower concentrations of component A, spherical particles of component A are dispersed in a matrix of component B, and

DOI: 10.1021/acs.iecr.7b05202
Ind. Eng. Chem. Res. 2018, 57, 4479−4504

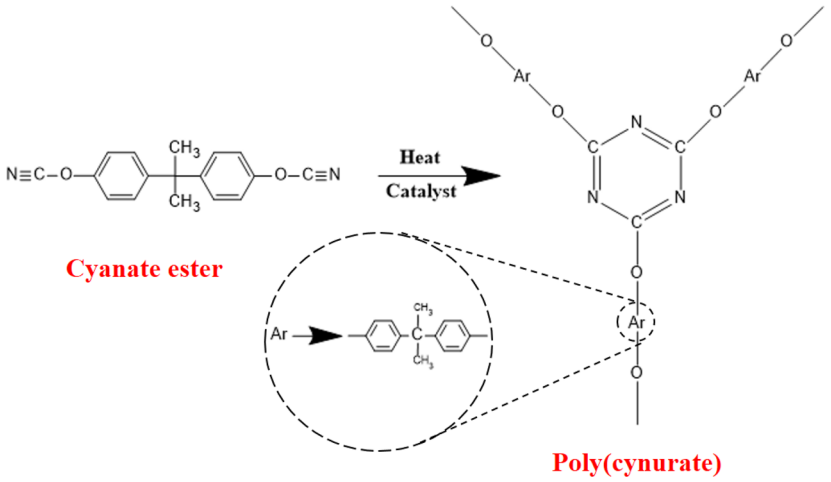

Figure 4. Cyclotrimerization of cyanate esters.

the resulting morphology is termed a particulate morphology, as shown in Figure 3a.

Although particles tend to take the spherical shape to minimize surface energy, other shapes are also possible, such as ellipsoids, platelets, etc. This phase separation is seen as shifting from a single-phase region to a metastable region in a phase diagram. In the metastable region of the phase diagram, phase separation occurs due to the NG mechanism, involving slow nucleation of component A followed by growth.[33]

An increase in the concentration of component A leads to a transition from the single-phase region into the spinodal region. Here, phase separation occurs by the SD mechanism and leads to co-continuous or phase-inverted morphology. Figure 3b shows the co-continuous morphology, in which both phases are continuous. This morphology is also termed as a "sea−island"-type morphology. With a further increase in the concentration of component A, phase inversion occurs, in which component A becomes the matrix and component B is dispersed in particle form, as shown in Figure 3c.

4. ELASTOMER VS THERMOPLASTIC TOUGHENING

Cyanate ester prepolymer has a reactive (−O−C≡N) functional group which on curing undergoes cyclotrimerization. The resultant three-dimensional cross-linked network is often called a poly(cyanurate), as shown in Figure 4.[4,46] The curing reaction is an addition polymerization reaction which does not form any byproducts. The CE homopolymers based on bisphenols have a T_g in the range of 250−290 °C, and for CEs based on novolacs, even higher T_g in the range of 270−350 °C or above are possible.[4] CEs possess excellent electric properties with a low dielectric constant (D_k = 2.66−3.08), which is unusual for equally high temperature resins. Even blending CEs with epoxies and BMIs has resulted in superior dielectric properties in the modified systems.[22,47] CEs are inherently tougher than epoxy and other high-temperature resins, and the fracture toughness of neat bisphenol A dicyanate (BADCy) resin is 0.62 MPa·m$^{1/2}$.[48] In order to enhance the toughness of CEs, two main approaches are popular. A number of studies are available for toughening of high-temperature epoxies with reactive elastomeric rubbers such as carboxyl-terminated butadiene−acrylonitrile (CTBN) copolymers.[49−54] This approach has also been extended to toughening of CEs without much success. Elastomer toughening causes significant improvement in the fracture toughness; however, a major drawback of this approach is that it causes degradation in high-temperature properties. Further, the addition of soft rubber in the stiff matrix reduces the overall yield strength and the modulus of system.[51]

Shaw et al.[55] blended CTBN with a BMI polymer system and reported an improvement in toughness only after 100 phr concentration of modifier. Such a high rubber loading causes degradation in the service temperature and modulus properties. Yang et al.[56,57] investigated toughening of CE resin using an experimental core−shell rubber modifier and reported a significant enhancement in toughness of the matrix.

Sachdeva et al.[58] investigated rubber toughening of high-temperature polyimide (PI) and reported a decrease in the T_g of PI from 300 to 137 °C. Unsaturation present in elastomeric structures like CTBN and amine-functionalized butadiene−acrylonitrile copolymer rubbers (ATBN) provides unwanted sites for reactions at high temperature.[58] Toughening of high-temperature polymers with particulate fillers like glass, silica, aluminum hydroxide, and zirconia also has been reported with limited success.[59,60]

On the other side, thermoplastics toughening of high-temperature thermosets resulted in significant improvements in fracture toughness without reducing their high-temperature properties.[61−68] As phase separation occurs while curing, individual components retain their T_g.[26,69] Marieta et al.[70] showed that CE and PEI, having T_g = 275 and 220 °C, respectively, retain their transition temperatures after blending at various concentrations such as 10, 15, and 20 wt% PEI. The phase-separated domain of the blend resulted in two T_g values, corresponding to the individual constituents in the blend. A slightly increase in T_g of PEI is reported for 15 and 20 wt% PEI blends. Thus, blending with thermoplastics having higher T_g results in an overall higher T_g of the blend system. Further, chemical resistance is also found to be improved for such systems.

Hedrick et al.[61,62] investigated blending hydroxy-functionalized poly(aryl ether sulfones) with epoxy resin at different molecular weights and reported improvement in fracture toughness. They showed that the addition of functionalized polysulfone (PSF) results in a two-phase particulate morphology, with particle size increasing with increase in molecular weight of the PSF. Hence, understanding the fundamentals associated with thermoplastic toughening and further its

DOI: 10.1021/acs.iecr.7b05202
Ind. Eng. Chem. Res. 2018, 57, 4479−4504

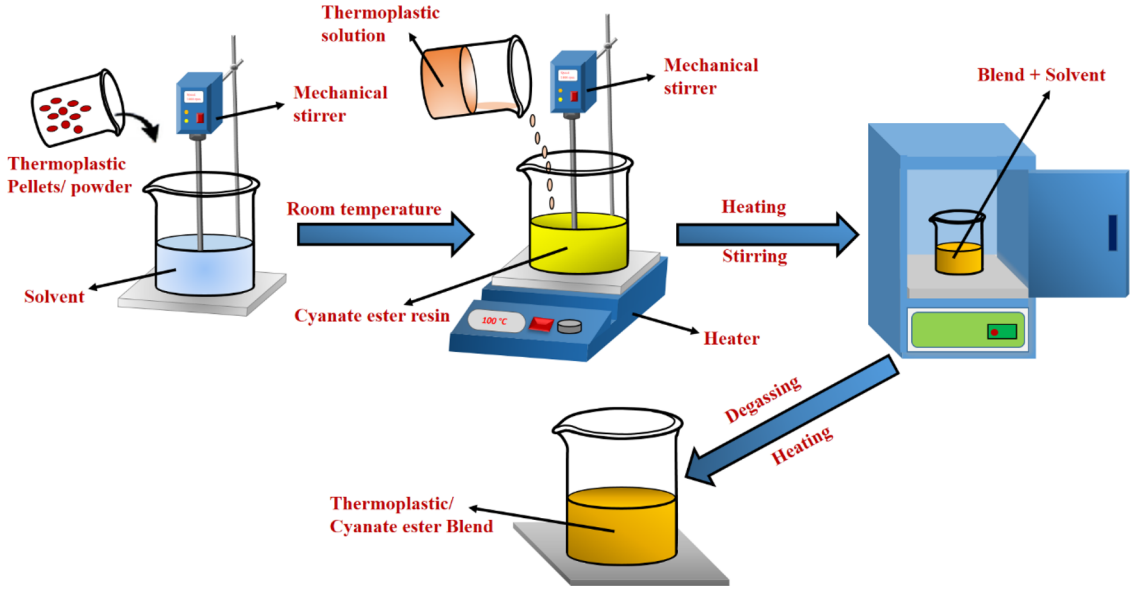

Figure 5. Schematic of solution blending process.

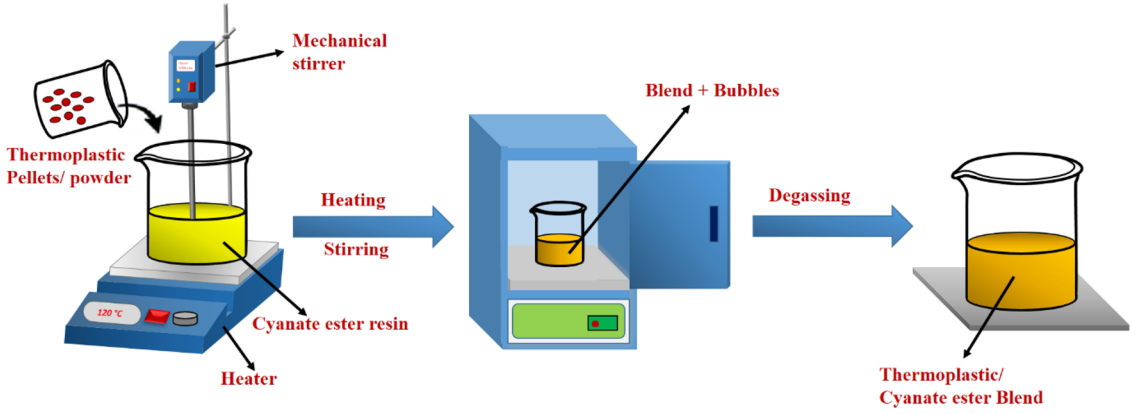

Figure 6. Schematic of solvent-free temperature-assisted solution mixing.

application in toughening of high-temperature thermosetting CEs became more important.

5. THERMOPLASTIC/CYANATE ESTERS BLENDING TECHNIQUES

Two main blending techniques, namely solution blending and solvent-free temperature-assisted solution mixing, are adapted for thermoplastic toughening of CEs. However, each of them has certain merits and demerits over the other.

5.1. Solution Blending. In the solution blending technique,[31,39,43] initially thermoplastics are dissolved in a solvent such as dichloromethane (CH_2Cl_2) to form a liquid solution. This liquid thermoplastic solution is then mixed with CE monomers/prepolymers at room temperature. The mixture is then continuously stirred, and heating is employed if necessary. The residual solvent is removed by the use of a vacuum along with heating to 90−120 °C, and catalyst is added if required. Figure 5 shows a schematic representation of the solution blending process. Solution blending is convenient and has been successfully implemented for blending of many thermoplastics, including PEI,[71] poly(ether sulfone) (PES),[72] etc.

Thermoplastic loadings of large quantities can easily be processed with solution blending.[73] However, removal of residual solvent imposes a great challenge, and 100% solvent removal is difficult to achieve. Further, an increase in viscosity of the solution with addition of thermoplastics imposes difficulty in the solvent removal process.

5.2. Solvent-Free Temperature-Assisted Solution Mixing. Amorphous thermoplastics like PSF, PEI, PES, polyacrylate, polycarbonate, etc. are miscible in CEs. This property of CEs can be utilized for obtaining blends of thermoplastics and CEs. In this process, pellets or a fine powder of thermoplastics is slowly added into liquid dicyanates such as AroCy L-10 with continuous stirring,[30] as shown in Figure 6. Liquid dicyanates are initially heated to a temperature of 100−130 °C.[26,30,74] If required, curing catalyst can be added during blending.[41] Complete mixing is ensured by observing transparency of the solution, and degassing is done to remove bubbles that form during mechanical mixing.

This process is extensively reported as "melt mixing", which typically refers to the process of melting the polymers and then mixing them to obtain homogeneous blends, and it utilizes specialized equipment like compounders, batch mixers, and extruders. Hence, this process cannot be corroborated technically as melt mixing. Therefore, the above blending

DOI: 10.1021/acs.iecr.7b05202
Ind. Eng. Chem. Res. 2018, 57, 4479−4504

process can also be termed as "solvent-free temperature-assisted solution mixing" based on its characteristics. Solvent-free temperature-assisted solution mixing is a most suitable blending technique for miscible thermoplastics up to approximately 20 wt%.[73] This advantage of "temperature-assisted solution mixing" makes the process more suitable for bulk production.

6. MORPHOLOGY AND MECHANICAL PROPERTIES OF THERMOPLASTIC-TOUGHENED CYANATE ESTERS BLENDS

The final morphology obtained after curing of thermoplastic-toughened cyanate blends is of great importance, as it controls the physical as well as mechanical properties of the end application. The morphologies obtained depend mainly on the thermoplastic composition, curing conditions, and molecular weight, allowing us to tailor the properties. Thus, a study of morphology and its variables becomes essential in the context of thermoplastic toughening of high-temperature thermosetting CE resins.

6.1. Poly(ether imide) (PEI) Blend. PEI has excellent mechanical and electrical properties. It has high service temperatures (up to 170−180 °C), low shrinkage, high moisture resistance, inherent flame retardancy, and low smoke emission during fire. Also, a low coefficient of thermal expansion (CTE) and a high dielectric resistivity are important properties of PEI. However, high cost and high density are the major drawbacks of this novel thermoplastic.[75]

6.1.1. Effect of Composition on Morphology. Harismendy et al.,[43,45] Tao et al.,[71] and Wang et al.[76] studied the effect of thermoplastic concentration on the final morphology obtained. For a composition of 5 wt% PEI, the particulate morphology is obtained. However, the spherical particles of PEI are very fine and can only be identified at higher magnification. Similar particulate morphology was obtained with a blend of 10 wt% PEI, in which spherical domains of around 0.5 mm diameter are dispersed in the cyanate-rich matrix, as shown in Figure 7a. This clearly shows that the degree of phase separation is higher for 10 wt% as compared to 5 wt% sample, and nucleated spherical particle thus grows in size. In this morphology, two particles size are observed, and in order to increase fracture toughness, bimodal distribution is preferred over unimodal distribution. This phase separation was attributed to the NG mechanism in which PEI phase nucleates and grows in cross-linking cyanate matrix during curing of the blend.[45]

A blend with 15 wt% PEI shows co-continuous morphology in which both the PEI and cyanate phases remain continuous. Also, small spherical particles of PEI and cyanate are dispersed in the cyanate-rich and PEI-rich phases, respectively, as shown in Figure 7b. This is attributed to secondary phase separation which occurred in already phase-separated PEI- and cyanate-rich domains. Adhesion of particles and matrix in the PEI-rich phase was poor, whereas the cyanate-rich phase showed good adhesion between particles. This is mainly because of the higher contraction of the thermosetting-rich phase compared to the thermoplastics-rich phase.[45]

Further increasing the composition up to 20 wt% leads to complete phase inversion, as shown in Figure 7c, in which cyanate appears as an independent spherical domain of around 2 mm diameter dispersed in PEI matrix. This co-continuous morphology shows broad particle size distribution. The phase separations for 15 and 20 wt% PEI concentration leading to co-continuous and phase-inverted morphology follow the SD

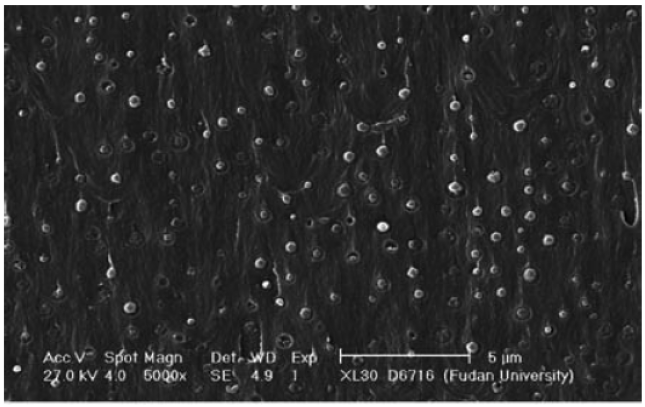

(a)

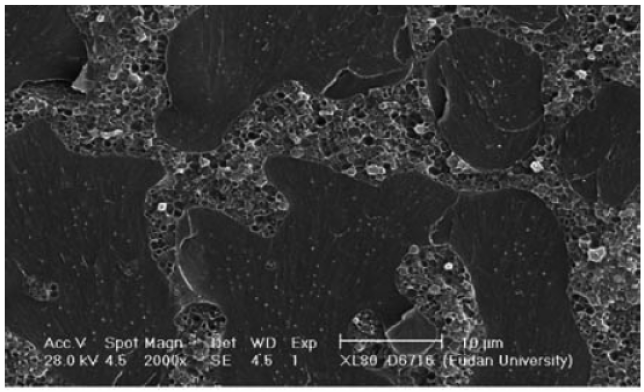

(b)

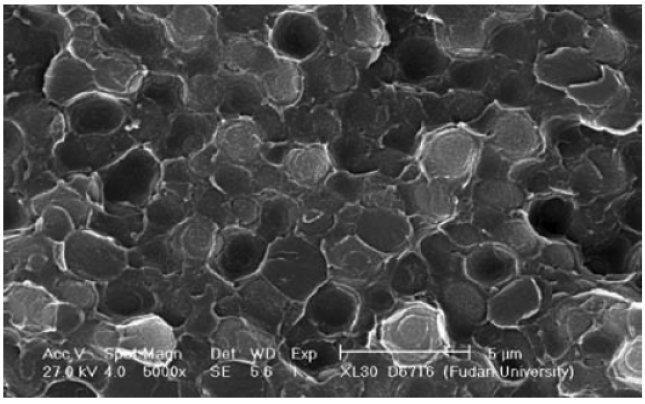

(c)

Figure 7. (a) Particulate morphology (10 wt% PEI). (b) Co-continuous morphology (15 wt% PEI). (c) Phase-inverted morphology (20 wt% PEI). Reprinted with permission from ref 76. Copyright 2006 Springer Nature.

mechanism, and 15 wt% composition is close to a critical point in the experimentally studied phase diagram.[39]

Examination of fracture toughness reveals that maximum toughening is achieved with 20 wt% PEI blend, which gives phase-inverted morphology. The main reason for the increment was ductile deformation of the thermoplastic matrix.[43,45] Also, the particulate morphology associated with 10 wt% PEI gave an almost 2-fold increase in toughness compared to neat cyanate resin.[45] This significant improvement is mainly because of the crack path deflection behavior of PEI spherical particles. Tensile study on blends concluded that addition of thermoplastics does not lead to significant changes in flexural properties, though the

DOI: 10.1021/acs.iecr.7b05202
Ind. Eng. Chem. Res. 2018, 57, 4479−4504

Table 1. Mechanical Properties of CE/PEI Blends with Varying PEI Concentrations and Molecular Weights

composition	tensile strength (MPa)	tensile modulus (GPa)	elongation at break (%)	compression strength (MPa)	K_{IC} (MPa·m$^{1/2}$)	G_{IC} (J/m^2)	refs
BADCy	63.7	2.27	4.14	327[b]	0.62[a]	100[a]	45, 71
BADCy/PEI(0.3) = 90/10	75.6	2.38	4.66	352[b]	1.35[a]	495[a]	45, 71
BADCy/PEI(0.3) = 85/15	84.7	2.39	5.86	427[b]	1.6[a]	680[a]	45, 71
BADCy/PEI(0.3) = 80/20	73.4	2.00	5.50	464[b]	3.1[a]	2480[a]	45, 71
BADCy/PEI(0.5) = 90/10	53.3	2.09	4.45				76
BADCy/PEI(0.5) = 85/15	62	1.98	4.45				76
BADCy/PEI(0.5) = 80/20	67.8	2.33	5.50				76

[a]Pre-curing at 180 °C for 3 h and post curing at 200 °C for 2 h, 250 °C for 1 h. [b]Pre-curing at 160 °C for 3 h and post curing at 200 °C for 2 h, 250 °C for 1 h.

co-continuous morphology obtained for 15 wt% PEI gives the maximum tensile strength, tensile modulus, and percent elongation at fracture.[71,76] Mechanical properties of cyanate/PEI blends are summarized in Table 1.

6.1.2. Effect of Curing Condition on Morphology. Harismendy et al.[45] studied the effect of curing temperature on morphology. Three different curing cycles, with pre-curing temperatures of 140, 160, and 180 °C for 3 h and post-curing at 200 °C for 2 h and at 250 °C for 1 h, were compared to determine their effect on the generated morphology of various blend compositions, varying from 0 to 20 wt%. Further, it was found that the activation energy for the curing reaction of CEs is independent of thermoplastic loading.[43] For the blend with 5−10 wt%, varying the curing temperature does not alter the overall morphology. However, the size of the spherical particles was found to increase with increasing curing temperature. The blend with 15 wt% PEI loading shows no significant change in morphology for the three temperatures cycles studied, and its phase separation mechanism remains the same. For 20 wt% PEI blend, 140 °C curing leads to globules of irregular sizes and shapes, but 180 °C curing generates higher average particle size distribution. Atomic force microscopy (AFM) study of the fracture surface reveals signs of ductile deformation of the thermoplastic matrix around particles.[45]

Fracture toughness was found to increase with increasing curing temperature for 5 and 20 wt% PEI, and it was exceptionally high for 20 wt% PEI pre-cured at 180 °C. This enhancement is due to the obtained bimodal distribution of particle sizes with small spherical particles and big globules. However, 10 wt% PEI showed a decrease in toughness with increasing pre-cure temperature, as particle size increased. For PEI with 15 wt% composition, the fracture toughness remains unaffected by changes in the curing conditions.

A similar trend was observed for the tensile test study, which shows that increase in tensile strength with increase in pre-cure temperature and for 20 wt% PEI blend, 180 °C pre-cure temperature results in highest tensile strength, as shown in Table 1.

6.1.3. Effect of Molecular Weight on Morphology. With increasing molecular weight, the viscosity of the blend also increases, thereby affecting phase separation during blend curing. Wang et al.[76] used two different PEIs having inherent viscosities of 0.3 and 0.5 dL/g with 6 h curing at 150 °C. The blend with 10 wt% PEI (0.5 dL/g) leads to a morphology different than particulate, in which a ribbon-like matrix domain of PEI is dispersed in the cyanate-rich matrix. Using 20 wt% PEI at 0.5 dL/g leads to smaller particle size than PEI at 0.3 dL/g at the same composition, mainly because the smaller cyanate particles are not able to merge further due to the increased viscosity of PEI with 0.5 dL/g sample.

Confirming the previous observations on morphology, 15 wt % PEI (0.3 dL/g), resulting in co-continuous morphology, showed the maximum tensile strength. Ribbon-like morphology is found to give minimum tensile strength, and hence, tailoring of the molecular weight of the modifier becomes essential, in order to avoid ribbon-like morphology.

6.2. Poly(ether sulfone) (PES) Blend. PES has high service temperatures up to 180 °C in an unstressed condition and good mechanical properties. It has fair shrinkage and moisture uptake properties. The broad range of service temperature, good creep behavior, and excellent electric properties are key features of this thermoplastic.[75]

6.2.1. Effect of Composition on Morphology. Recently, in 2013, Thunga et al.[26] evaluated toughness and CTE behavior as a result of blending with PES at different compositions. Up to 15 wt% of PES, the morphology observed was particulate, in which finely dispersed PES particles were found inside a continuous bisphenol E cyanate ester (BECy) phase. Increasing concentration from 5 to 15 wt% PES resulted in an increase in size and number of PES particles along with a simultaneous decrease in cyanate phase. This morphology with continuous BECy phase changes to a discontinuous structure at 20 wt% PES, which is called a co-continuous phase. With PEI only 15 wt% loading resulted in co-continuous morphology, but here with PES, a larger loading of up to 20 wt% is required to achieve a similar morphology. This requirement of higher PES loading as compared to PEI is mainly due to the lower molecular weight of PES as compared to PEI. However, instead of the phase-inverted morphology obtained at higher concentrations of PEI, 30 wt% PES led to a non-uniform phase-separated morphology in which large BECy micro-domains are distributed inside the separated BECy/PES structure.

Evaluation of flexural properties using a three-point bending test concluded that flexural stress, flexural strength, and flexural toughness increase initially up to 10 wt% PES, leading to particulate morphology, and then decrease with further increase in PES concentration. Kinloch et al.[69] examined the fracture toughness properties and results of mechanical properties of a PES/CE blend, which are listed in Table 2. The decrease in

DOI: 10.1021/acs.iecr.7b05202
Ind. Eng. Chem. Res. 2018, 57, 4479−4504

Table 2. Mechanical Properties of PES-Toughened Cyanate Ester Blend

composition	flexural stress (MPa)	flexural strain (MPa)	flexural toughness (MPa)	fracture energy (J/m^2)	refs
0 wt% PES	110.8[a]	6[a]	349[a]	150[b]	26, 69
5 wt% PES	128[a]	8.7[a]	735[a]		26
10 wt% PES	131.7[a]	8[a]	638[a]	190[b]	26, 69
15 wt% PES	118[a]	7.7[a]	600[a]		26
20 wt% PES	92[a]	4.5[a]	199[a]	379[b]	26, 69
25 wt% PES				330[b]	75
30 wt% PES	59[a]	2.15[a]	51[a]	340[b]	26, 69

[a]Pre-cured at 180 °C for 2 h and post-cured at 250 °C for 2 h. [b]Fractured at 21 °C.

flexural properties at higher concentration (20−30 wt%) is due to a discontinuous BECy phase. However, the CTE was found to decrease with increasing PES concentration, as PES has a considerably lower CTE (~25 ppm/°C) than BECy (~60 ppm/°C) at room temperature. A low value of thermal expansion coefficient is essential for high-temperature polymer composites to improve dimensional stability and avoid residual thermal stress in composites.[26]

When PESs are functionalized and blended with CEs, they exhibit improved properties. Chang et al.[30] used hydroxyl- and cyanate-terminated poly(ether sulfone)s, denoted as HPES and CPES, respectively, for toughening of BADCy. Two PES compositions, 10 and 50 wt%, giving particulate and co-continuous interconnected structures, respectively, were evaluated for fracture toughness with and without using curing catalyst. Surprisingly, the 10 wt% blend of CPES resulted in blurring the interface with particulate morphology, as shown in Figure 8a.

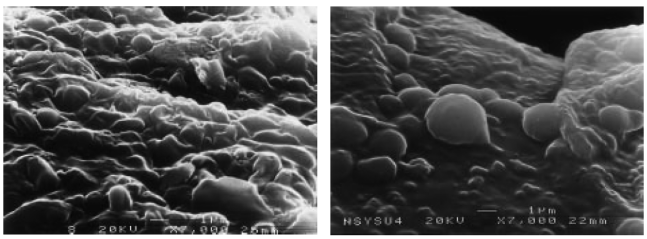

(a) (b)

Figure 8. Morphology of 10 wt% PES having different functional groups: (a) CPES and (b) HPES with 1 wt% catalyst. Reprinted with permission from ref 30. Copyright 2000 Elsevier.

This blurring interface is a result of interaction between BADCy and CPES due to polycyclotrimerizations by inherent cyanate groups present in both monomers. This blurring interface causes an improvement in adhesion between particles and matrix. As HPES does not have a cyanate group, no blurring interface was observed. But, as shown in Figure 8b, the use of 1 wt% catalyst reveals the existence of the blurring interface due to inter-reaction between the hydroxyl termini in HPES and the cyanate group in BADCy, which is promoted by the catalyst, thus improving mechanical properties, as listed in Table 3.

6.2.2. Effect of Molecular Weight on Morphology. Rau et al.[77] evaluated the influence of different molecular weights of hydroxyl-functionalized phenolphthalein-based poly(arylene ether sulfone) on the morphology of the PES/CE blend.

Table 3. Effect of Functional Group and Curing Catalyst on Mechanical Properties

composition	tensile strength, σ (MPa)	tensile modulus, E (GPa)	fracture energy, G (J/m^2)	ref
10 wt% HPES	81.97	3.15	33.5	30
50 wt% HPES	78.85	2.82	138.5	30
10 wt% HPES with curing catalyst	81.97	3.15	67	30
50 wt% HPES with curing catalyst	78.85	2.82	415.6	30
10 wt% CPES	81.98	3.16	80.3	30
50 wt% CPES	78.89	2.82	416.6	30

Two PESs, with number-average molecular weight M_n = 15 000 and 20 000 g/mol, were used to modify CEs at varying compositions from 20 to 30 wt% PES. For M_n = 15 000 g/mol, 20 wt% PES resulted in co-continuous morphology, and increasing the concentration to 30 wt% led to a finer phase structure. However, increasing the molecular weight to M_n = 20 000 g/mol for similar 20 wt% PES concentration was found to generate phase-inverted morphology. Zhan et al.[31] found a similar effect when the intrinsic viscosity of PES was increased in a cyanate/epoxy/PES blend. Thus, higher viscosity at the onset of phase separation, due to an increase in molecular weight, can achieve co-continuous or phase-inverted morphology even at a lower concentration of modifier. Recently, Uhlig et al.[78] studied four different molecular weights of PES to modify two different grades of CEs. BADCy and METHYLCy were modified using PES at varying molecular weights. It was found that increasing molecular weight increases fracture toughness in both CEs, and higher toughening was achieved with co-continuous morphology obtained at 20 and 25 wt% PES.

6.3. Polysulfone (PSF) Blend. PSFs have a broad range of service temperature from −100 to +200 °C, and they are known for their excellent mechanical and electrical properties, fatigue endurance, fair shrinkage, and water uptake properties. Continuous exposure to high service temperature up to 150 °C is common for PSF thermoplastics. Additionally, their moisture and hot water resistance properties are remarkable, with no hydrolysis.[75]

6.3.1. Effect of Composition on Morphology. Study on CE blend with PSF was first reported by Woo et al.[73] in 1994. Morphology study reveals that there is a transition of from particulate morphology to co-continuous at 20 wt% concentration. Further, Hwang et al.[48] investigated functionalized PSF for its effect on toughening of CEs in 1997. PSFs were functionalized via bromination and cyanation reaction to result in cyanated polysulfone (CN-PSF), and both PSF and CN-PSF were solution blended with BADCy in three different concentrations of 10, 20, and 30 phr. For PSF concentration of 10 phr, particulate morphology was observed, with spherical particles having a size of around 0.5−1.0 μm dispersed in the BADCy matrix. Increasing PSF concentration to 20 phr led to phase inversion, where the size of dispersed BADCy particles was around 4−8 μm. Further increasing concentration to 30 phr does not alter the morphology, but the size of BADCy particles is reduced to 1−2 μm due to increased viscosity of the blend suppressing the growth of particles.

For CN(0.6)-PSF blend, smaller particle size of 0.2−0.3 μm was observed for 10 phr, and an increase in concentration to 20 phr generates co-continuous morphology. Further increasing

DOI: 10.1021/acs.iecr.7b05202
Ind. Eng. Chem. Res. 2018, 57, 4479−4504

Table 4. Mechanical Properties of Neat PSF and CN-PSF at Varying Concentrations

composition	flexural strength (MPa)	flexural strain (%)	flexural modulus (MPa)	K_{IC} (MPa·m$^{1/2}$)	ref
BADCy	195.97 ± 3.7	7.4 ± 0.3	3112 ± 51	0.62	48
BADCy/neat PSF (10 phr)	185.4 ± 7.3	6.9 ± 0.6	3107 ± 64	0.825	48
BADCy/neat PSF (20 phr)	183.8 ± 9.0	4.5 ± 0.2	3200 ± 114	1.125	48
BADCy/neat PSF (30 phr)	130.8 ± 2.9	4.5 ± 0.2	3106 ± 51	1.25	48
BADCy/CN(0.6)-PSF (10 phr)	166.5 ± 7.5	7.3 ± 1.2	2789 ± 61	0.78	48
BADCy/CN(0.6)-PSF (20 phr)	149.6 ± 12.5	5.8 ± 0.8	2844 ± 69	1.14	48
BADCy/CN(0.6)-PSF (30 phr)	141.3 ± 3.6	5.0 ± 0.2	2887 ± 61	1.52	48

concentration to 30 phr causes phase inversion, but the particle size observed was small, 0.3−0.4 μm. Also, adhesion between particles and matrix was found to be good for observed morphology. This change in morphology and reduction in particle sizes are due to the chemical reaction of the functional group in CN-PSF with the cyanate group.

Fracture toughness evaluation highlighted that a blend of CN-PSF with 30 phr concentration has a maximum toughening effect due to tough CN-PSF acting as matrix, and chemical reaction helps in improving adhesion between particle and matrix. Interestingly, 20 phr concentration for both cases leads to equal toughening, as the morphologies observed are different, where CN-PSF blend leads to co-continuous morphology while PSF blend leads to phase inversion morphology.

6.3.2. Effect of Curing Condition on Morphology. Changes in morphology as a result of different curing conditions were studied by Hwang et al.[29] in 1999. Observation of morphology revealed that the change in phase separation mechanism was a function of curing temperature for the BADCy/PSF blend. For curing temperature of 250 °C, particulate morphology with PSF particles dispersed in BADCy phase was observed for 10 phr, which changed to co-continuous at 15 and 20 phr concentration, followed by phase inversion at 30 phr. However, decreasing the curing temperature to 200 and 230 °C changed the phase separation mechanism, even at 20 phr concentration, and resulted in phase inversion, in which BADCy particles are dispersed in the PSF matrix phase. Further, BADCy particle size reduces with increasing concentration to 30 phr. This reduction in BADCy particle size is due to an increase in viscosity with a decrease in curing temperature constraining the growth of particles. For a low curing temperature of 80 °C, only 10 phr of PSF concentration formed a co-continuous morphology, which changed to phase inversion at only 15 phr.

Marieta et al.[79] used AFM to study morphology changes as a result of different pre-cure temperatures. For 15 wt% bisphenol A PSF, the transition from particulate morphology to dual-phase morphology consisted of both particulate and co-continuous phases, which were observed with increasing pre-cure temperature from 160 to 180 °C. Also, AFM images revealed a secondary phase separation that occurs in the separated thermoplastic domain.

6.3.3. Effect of Molecular Weight on Morphology. Molecular weight causes changes in morphology due to the fact that viscosity increases as the molecular weight of the modifier increases. Hwang et al.[72] in 2000 studied the effect of four different molecular weights on morphology. Initially, at low molecular weight, for samples with 10 phr concentration, morphology was particulate, having PSF particles dispersed in BADCy matrix. At the same concentration, increasing the molecular weight led to an increase in size of PSF particles, and at a higher molecular weight of around M_w = 84 400, the phase changed to co-continuous morphology. Thus, with higher molecular weight, only 15 phr concentration can cause phase inversion, and this change is driven by viscosity change.

6.3.4. Mechanical Properties of Cured Blend. Table 4 shows that the fracture toughness of neat BADCy was improved as a result of adding PSF. For the neat PSF as well as CN-PSF, the maximum value of fracture toughness was obtained for 30 phr concentration. However, CN-PSF gives maximum toughening due to the functional group present which reacts and improves the adhesion between particles. Woo et al.[73] compared two thermoplastics, PEI and PSF, at 20 wt% in polycyanate and concluded that PSF is more effective in toughening, due to the observed small particle size of approximately 0.8 μm compared to PEI particles, which are 2 μm or greater in the co-continuous phase. The fracture toughness, K_{IC}, for 20 wt% PSF/polycyanate was 1.45 MPa·m$^{1/2}$, much higher than that of PEI, K_{IC} = 1.10 MPa·m$^{1/2}$, at the same concentration. However, the T_g of PSF is lower compared to PEI, i.e., T_g < 200 °C.

Flexural properties of BADCy are found to degrade as a result of blending with PSF. This is due to the fact that neat PSF has a lower flexural strength of 127.6 MPa as compared to neat BADCy.[48]

6.4. Poly(arylene ether) Blends. Poly(arylene ether) blends are high-performance engineering thermoplastics with service temperature up to 250 °C in unstressed conditions. They have excellent mechanical properties with high modulus and hardness. They also have good chemical and electrical properties, good creep behavior, and good fatigue properties along with fair resistance to moisture.[75]

6.4.1. Effect of Curing Condition on Morphology. Blends with various concentrations of reactive thermoplastics, like hydroxyl-functional phenolphthalein-based amorphous poly(arylene ether ketone), poly(arylene ether sulfone), and poly(arylene ether phosphine oxide), have been reported to have a toughening effect as a result of blending with CEs. Srinivasan et al.[80] evaluated the effect of curing cycles on morphology and the corresponding effect on toughness of the blends. They reported that morphology changes from particulate at 10 wt% to phase-inverted at 30 wt%, with co-continuous at 20 wt% loading of modifier. For a blend of phenolphthalein-based hydroxyl-functionalized poly(arylene ether sulfone) (PPH-PSF-OH) with 25 wt% in CEs, initially co-continuous morphology was obtained for a curing cycle of 1 h at 104 °C, which changed to finer phase morphology upon holding 5 h at the same temperature. Evaluation of fracture toughness concluded that a morphology that exhibits the finer texture phase-separated domain results in lower fracture toughness. The blend of poly(arylene ether phosphine oxide) (PPH-PEPO-OH) with CEs does not show a preferential staining in scanning electron microscopy (SEM), which is attributed to the development of a phase-mixed network, which

DOI: 10.1021/acs.iecr.7b05202
Ind. Eng. Chem. Res. 2018, 57, 4479−4504

is further confirmed by a single peak in dynamic mechanical analysis.[81]

Table 5 shows the fracture toughness of all three poly(arylene ether) blends at various concentrations. The more

Table 5. Fracture Toughness of Poly(arylene ether) Modifiers at Varying Concentrations in Cyanate Esters

	K_{IC} (MN/m$^{3/2}$)			
concentration	M_n = 15 000 PPH-PEPO-OH	M_n = 15 000 PPH-PEK-OH	M_n = 15 000 PPH-PSF-OH	ref
0 wt%	0.53	0.53	0.53	80
10 wt%	0.61	0.7	0.8	80
20 wt%	0.7	0.9	1.21	80
30 wt%	0.8	1.3	1.87	80

distinguished phases and morphology of poly(arylene ether sulfone) blend result in higher fracture toughness for all concentrations compared to other poly(arylene ether) modifiers. For 30 wt% PPH-PSF-OH, the maximum toughening is observed, with K_{IC} = 1.87 MN/m$^{3/2}$. The poly(arylene ether ketone) (PPH-PEK-OH) blend resulted in intermediate toughening with respect to the other modifiers.

6.4.2. Effect of Molecular Weight on Morphology. Toughening of CEs as a result of blending with poly(arylene ether sulfone) at various molecular weights was reported by Srinivasan et al.[81] in 1998. The study revealed that both chemistry and the molecular weight of the modifier are important to control the morphology and to result in a higher toughening effect. Table 6 summarizes the fracture toughness for different molecular weights of poly(arylene ether sulfone) blends at different concentrations in CEs.

Table 6. Fracture Toughness of Poly(arylene ether sulfone)/Cyanate Ester Blend at Varying Molecular Weights

	K_{IC} (MN/m$^{3/2}$)			
concentration of poly(arylene ether sulfone)	M_n = 10 000	M_n = 15 000	M_n = 20 000	ref
0 wt%	0.53	0.53	0.53	81
10 wt%	0.55	0.8	0.9	81
20 wt%	0.62	1.2	1.25	81
30 wt%	0.95	1.83	2.05	81

It can be seen that the low molecular weight of M_n = 10 000 results in insignificant improvement in fracture toughness. Study of its fractured surface gives evidence about the absence of texture, signifying no multi-phase network formation. The highest molecular weight of M_n = 20 000 resulted in maximum toughening, followed by intermediate improvement with M_n = 15 000. This improvement with higher molecular weight was due to higher degrees of phase separation, which leads to a larger domain in morphology. Again, a higher concentration of modifier with phase-inverted morphology leads to the highest toughening of the matrix.

6.5. Other Thermoplastics Blends. Harvey et al.[82] studied polycarbonate blends with CEs and concluded that no phase separation occurred through characterization using small-angle laser light scattering and differential scanning calorimetry. Further, the T_g for such a blend lies midway between the T_g values of the two individual polymers. However, no mechanical evaluation was reported to conclude on toughening of the base matrix. Iijima et al.[41] blended poly(ethylene phthalate) (PEP) with CEs to improve toughness. They reported that the homogeneous solution formed with PEP and resulted in phase separation after curing. The observed morphology showed fine PEP particles of size less than 1 μm dispersed in cyanate matrix for 20 wt% of PEP of low molecular weight (MW = 13 600); further increase in molecular weight resulted in increased particle size. Fracture toughness (K_{IC}) study concluded that 20 wt% PEP (MW = 19 800) results in a 120% improvement in fracture toughness. Also, flexural properties of these modified systems were equal or a little higher as compared to those of the unmodified system. However, a slight decrease in T_g was observed as a result of blending with PEP. The modification also resulted in increased water absorption in this modified system. Fainleib et al.[83] evaluated blending of CEs with hydroxyl-terminated polyethers such as polyoxypropylene (PPG) and polyoxytetramethyl glycol (PTMG). Even loading >10 wt% PPG resulted in tensile strength of around 30−35 MPa and glass transition value above 250 °C. Improvement in tensile properties was observed up to a concentration of 40 wt %, and further addition of modifier led to a decrease in tensile properties of the matrix. Iijima et al.[84] synthesized random as well as multi-block-type PIs and blended them with CEs. They concluded that random PIs are more effective in toughening than multi-block-type PIs. Further, co-continuous and phase-inverted morphology resulted in effective modification of CEs. A blend of 15 wt% random PIs (MW = 63 400) resulted in an almost 65% increase in fracture toughness without degrading flexural modulus and T_g.

Puglia et al.[85] reviewed the effectiveness of hybrid modification of epoxy with microscale elastomer/thermoplastic and nanoscale fillers such as silica, carbon nanotubes, clay, etc. They concluded that hybrid modification in epoxy made it possible to tailor multiple properties independently at two length scales, i.e., nanoscale filler and microscale thermoplastic/elastomer, thus extending their range of applications. This hybrid modification provides an effective way to balance between toughness and modulus properties along with imparting excellent thermal and moisture stability in the epoxy resin. This hybrid modification can also be extended for these thermoplastic-toughened CE blends to enhance their properties further. Filler modification of cyanate resins have been studied by various researchers.[86−88] Badrinarayanan et al.[89] incorporated zirconium tungstate in CEs to enhance the dimensional stability, as zirconium tungstate has a negative CTE. They reported that modified CE resin resulted in a decrease in the CTE of the matrix, and hence reduced the warpage and curvature in fiber-reinforced composites, thereby minimizing residual stress. In another study, Pan et al.[90] modified CE resin with silicate nanorods and reported a 40% increase in the modulus. Further, strength and toughness were increased to 42 and 55%, respectively. Wooster et al.[91] studied hybrid modification of CEs with silica filler and both elastomer and thermoplastic modifiers and reported an increase in toughness. Xie et al.[92] evaluated the effect of a hybrid filler, CTBN rubber/silicon nitride (CTBN/Si_3N_4), in the BADCy resin and reported about 59.5% increase in impact strength. Also, flexural strength was increased by 34.3% for the hybrid modified system. Thus, hybrid modification of CE blends is an another effective method to enhance the properties of matrix, thereby extending their applications.

DOI: 10.1021/acs.iecr.7b05202
Ind. Eng. Chem. Res. 2018, 57, 4479−4504

7. TOUGHENING MECHANISMS IN THERMOPLASTIC-TOUGHENED CYANATE ESTER BLENDS

Understanding the mechanism of toughening is important, as it allow one to design properties by controlling various decisive factors such as particle size, volume fraction, modulus, etc. Phase separation occurs in thermoplastic-toughened thermoset resins, producing two-phase morphology, following various toughening mechanisms based on the characteristics of the polymer used. Commonly reported toughening mechanisms for these blends are crack pinning, crack path deflection, crack bridging, stress whitening and debonding, cavitation, plastic hole growth,[93] etc., which are further discussed in detail here.

7.1. Crack Bridging. Crack bridging is the most probable mechanism in thermoplastic-toughened resins, where the phase-separated rigid particles span the two crack surfaces and reduce the stress concentration by applying surface traction at the crack tip.[94] Energy absorbed by the crack-bridging particles increases the toughness. Figure 9 gives a schematic representation of crack bridging in which cracks propagate in a brittle matrix through particles without breaking them. With the opening of crack, these particles span the crack surfaces, and energy absorbed in stretching and tearing of bridging particles leads to toughening.

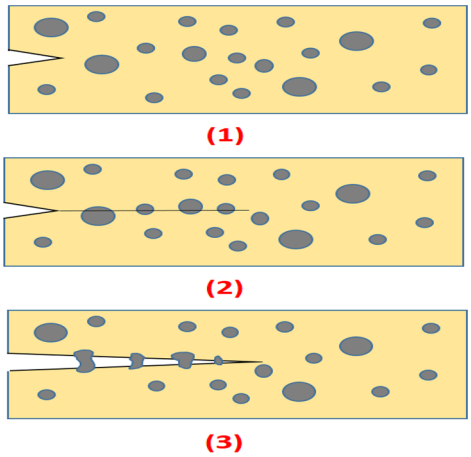

Figure 9. Schematic showing stages of the crack bridging mechanism.

In the fractographs, the fractured surface showing damaged particles in the plane of the crack gives evidence for toughening by the crack bridging mechanism. Several studies on thermoplastic-toughened epoxy have reported crack bridging as a major toughening mechanism.[61,64,65] Also, crack bridging is independent of the potential of the matrix for plastic deformation.[95] Kunz-Douglass et al.[96] studied rubber toughening of epoxy resin and proposed a model for crack bridging. They observed that when the crack propagates, it leaves rubber ligaments attached to the crack surface and stretches with opening of the crack wedge, thereby acting like a spring. Based on their observation, those researchers proposed the first model to quantify toughening based on the amount of elastic energy stored in the rubber particles during stretching. This model considers three major factors that lead to toughening: (1) particle size, (2) particle tearing energy, and (3) volume fraction of particle in the matrix.

According to rule of mixture, the toughness of a composite can be expressed as follows:

$$G_{IC} = G_{IC}^{M}(1 - V_p) + \Delta G_{IC} \quad (5)$$

where G_{IC}^{M} is the fracture toughness of the matrix, V_p is the volume fraction of particles, and $\Delta G_{IC} = 4\Gamma_t V_p$ represents the increase in fracture toughness due to bridging particles, where Γ_t is the tear energy of the particle (the smaller the particle, the higher the tearing energy).

Kinloch et al.[97] disagreed with the above theory, as it does not consider stress whitening, large plastic deformation, increase in toughness at elevated temperature, etc. Also, rubber tear theory does not explain how nonreactive rigid thermoplastic particles can lead to toughening, as they possess a low deformation characteristic. They proposed another a model, which considers matrix dilatational deformation and cavitation caused by rubber particles as a primary toughening mechanism. Their observation concluded that the major rubber-toughening achieved with the epoxy was due to plastic deformation of the matrix. Based on Kinloch's work,[8] Huang et al.[98] developed a mathematical model to assess the toughening due to crack bridging as well as cavitation and shear banding. According to the Kinloch model,[97] fracture energy of rubber-toughened epoxy is given by the following equation:

$$G_{IC} = G'_{IC} + \Psi \quad (6)$$

where G'_{IC} is the fracture energy of unmodified epoxy resin, Ψ is the toughening due to rubber particles, $\Psi = \Delta G_r = \Delta G_s + \Delta G_v$, where ΔG_r is the toughening due to crack bridging ($\Delta G_r = 4\Gamma_t V_p$, given by the rubber tearing strain model proposed by Kunz-Douglass[96]) and ΔG_s and ΔG_v are toughening contributions due to plastic shear banding and plastic void growth in the matrix, respectively. For the calculation of ΔG_s and ΔG_v, Kinloch et al.[51,97,99] proposed a plastic shear-band mechanism.

Thus, using the above model, various aspects of toughening such as particle size, volume fraction, and fracture strength of particles can be designed effectively. However, these model are proposed for rubber particles, and their applicability for thermoplastic toughening still remains questionable due to the different physical properties of the particles.

7.2. Crack Pinning. In this mechanism, rigid thermoplastic particles act as a crack arrester, causing the crack to blow out and thus to absorb extra energy. This is a common mechanism for a morphology containing a dispersion of thermoplastic particles rather than a brittle thermoset in particulate form, as thermoplastics are tough and impenetrable.[99] In the crack pinning mechanism, the fracture surface consists of a "tail" near the particle, which can be observed in fractographs. A schematic representation of crack pinning mechanism is shown in Figure 10. When the moving crack meets the inhomogeneity in the path, the crack temporarily gets pinned at that point. The front of the pinned crack then bows forward between pinning particles, until it forms semi-circular segments with diameter equal to the spacing between pinning points. An overlapping segment will result behind the pinning points, thereby breaking the crack front, as shown in Figure 10. Thus, energy absorbed during the time of crack pinned until the breaking of the crack front behind the pinning points leads to toughening via the crack pinning mechanism.

In 1970, Lange[95] reported a crack pinning mechanism in which secondary phase inhomogeneities act as obstacles impeding the front of the moving crack, requiring more energy for propagation. In their study, aluminum trihydrate filler was added in the epoxy as a fire-retarding filler, which simultaneously led to an increase in fracture toughness, and

DOI: 10.1021/acs.iecr.7b05202
Ind. Eng. Chem. Res. 2018, 57, 4479−4504

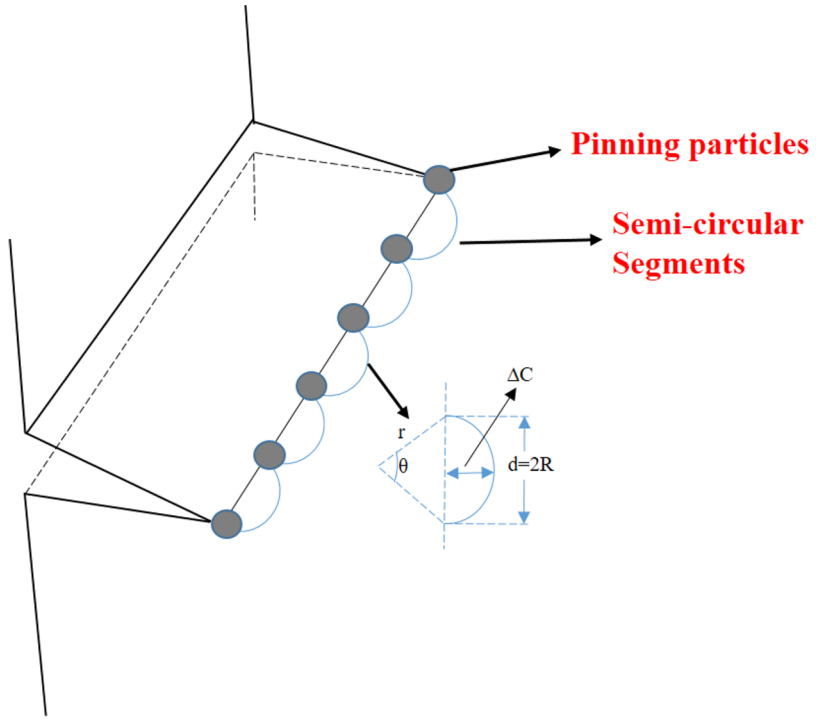

Figure 10. Schematic of the crack pinning mechanism.

increments were found to depend on the volume fraction of the fillers. To explain the model fractographs were studied, and it was stated that a crack initiates in the brittle matrix which interacts with a second phase particle, bows between filler particles, but remains pinned. Their model gives a functional relationship between the fracture energy of filler-modified material and the average spacing between the filler particles. According to their model, the fracture energy in filler-modified composite is given by the following equation:

$$G_c = 2\left(\gamma_0 + \frac{T}{d}\right) \tag{7}$$

where T is the line energy per unit length of crack front and d is the arc of the circle (i.e., distance between inhomogeneities, $d = 2R$). Crack pinning is mainly associated with inorganic rigid filler particles and is less effective in ductile matrix materials.[98] Another model was proposed by Evans,[100] which accounts for the segment interaction of crack front and predicts the nonlinear increase in fracture toughness, which is a function of the volume fraction of particles. Kinloch et al.[99] reported about the crack front bowing when the epoxy resin was modified with glass particles. Yee[101] investigated toughening of nylon-66 with rigid polyphenylene oxide particles and found that rigid particles induced localized dilatation and matrix deformation, which are the major reasons for toughening. Also, cavitation and crack pinning by the rigid particle increasing stress concentration at the crack tip contribute significantly.

7.3. Crack Path Deflection. Crack path deflection is the mechanism associated with rigid secondary phase particles dispersed in a brittle matrix. In this mechanism, the rigid thermoplastic particles cause the crack to deviate from its path into another plane. This crack path deviation results in increased surface area and, hence, the energy required for propagation of the crack. The crack path deflection mechanism is schematically represented in Figure 11.

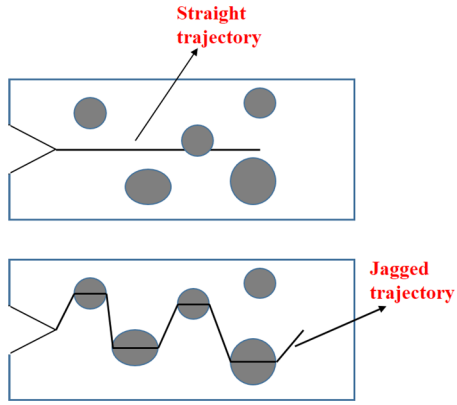

Figure 11. Schematic representation of the crack path deflection mechanism.

Kinloch et al.[102] reported about crack path deflection as a toughening mechanism for particulate morphology in thermoplastic-modified epoxy systems. Faber et al.[103] proposed a quantitative model for crack path deflection which assumes particle size has no effect on path deflection. Their model is based on the fact that, when the crack intercepts the second phase particle, it will tilt at an angle of θ from its original plane, the angle of tilt depending upon the position of the particle with respect to the path of the advancing crack, as shown in Figure 12a. If an adjacent particle causes the crack to tilt back in the opposite direction, the crack front will twist, as shown in Figure 12b.

Thus, this tilting and twisting of the crack results in a mixed mode of loading. The tilted crack represents Mode I (opening) and Mode II (sliding) loading, while the twisted crack has Mode III (tearing) loading along with Mode I. Using these loading conditions and local stress intensities at the crack front, Faber[103] proposed the equation for fracture toughness given by

DOI: 10.1021/acs.iecr.7b05202
Ind. Eng. Chem. Res. 2018, 57, 4479−4504

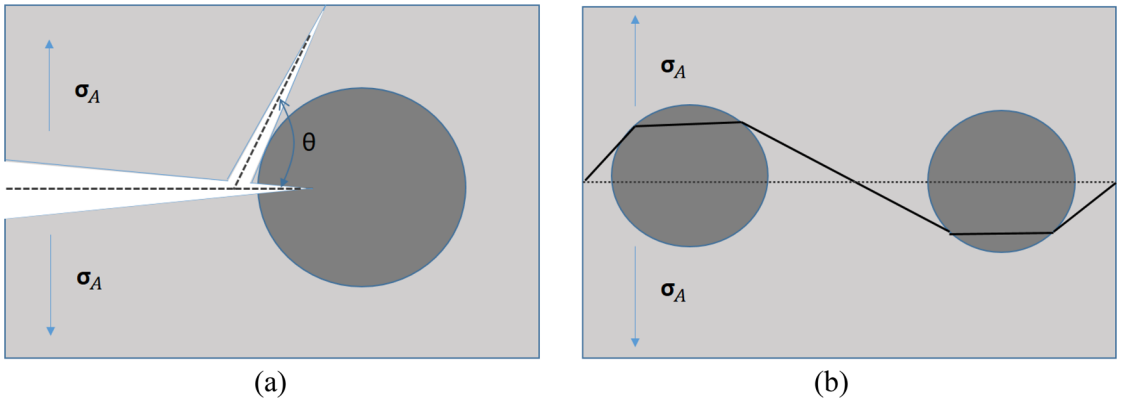

Figure 12. Tilt and twist of crack due to interaction with particles.

$$G_c = \left(\frac{G^m}{G}\right) G_c^m \tag{8}$$

where G is the average strain energy release rate representing the net crack driving force and G^m is the strain energy release rate for undeflected crack. Based on this study, Faber concluded that twisting of the crank front is important and contributes significantly in toughening.

7.4. Cavitation and Massive Shear Yielding Mechanism. This mechanism is associated with blunting of the crack tip due to its interaction with a cavity developed around the second phase particle in the matrix. This interaction of crack front with the cavity relieves the tri-axial tension state to a more uniaxial tensile stress state, and this new stress state favors shear band formation, creating a large plastic zone.[104,105] Most of the studies on rubber toughening of epoxy reported that cavitation around the rubber particles, which leads to crack blunting and plastic deformation, is the primary toughening mechanism.[105,106]

Pearson et al.[105] investigated the deformation of CTBN-modified epoxy resin in a three-point bending test and concluded that cavitation of the rubber particles was the primary toughening mechanism present. Observation under optical microscope revealed shear bands, which were generated due to cavitated particles. Gazit et al.[106] studied reactive rubber toughening in epoxy resin and reported that a micro-cavitation process resulted in toughening of the epoxy. In tensile testing, micro-cavitation was observed throughout the sample gauge length. Also, stress whitening and shear band formation were observed in the sample tested on a tensile impact tester, as shown in Figure 13.

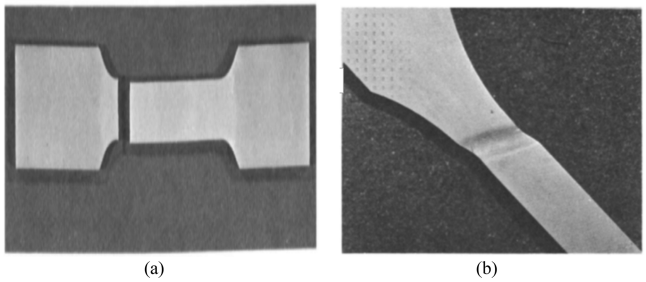

Figure 13. Tensile impact test sample: (a) stress whitening and (b) shear band formation. Reprinted with permission from ref 106. Copyright 1983 American Chemical Society.

It has been reported that light scattering from the cavitated particles results in stress whitening, which is often observed at the crack tip or at the fracture surface.[101,107] Stress whitening has also been reported in thermoplastic-modified systems in a few references.[98]

Dompas et al.[104] proposed a model for rubber particle cavitation which assumes spherical rubber particles and hydrostatic tension on the particle acting as driving force for cavitation. They concluded that particle cavitation is a function of relative volumetric strain given by the following equation:

$$d_o = \frac{12(\gamma_r + \Gamma_{sc})}{K_r \Delta^{4/3}} \tag{9}$$

where Δ is the relative deformation of particle, K_r is the bulk modulus of rubber, Γ_{sc} is the energy per unit area, and γ_r is the van der Waals surface tension of rubber. From the above equation it is clear that larger particles will cavitate first in the deformation process, followed by smaller particles.

7.5. Toughening Mechanisms in Thermoplastics-Modified Cyanate Ester Blends. The toughening mechanism in any system is complex and often consists of multiple mechanisms working simultaneously. McGrail et al.[108] reported that crack path deviation and crack front pinning are the toughening mechanisms in particulate/co-continuous/phase-inverted morphologies. Their study was based on reactively terminated PSF and CE, epoxy, and BMI blends. DiBerardino et al.[27] studied the toughening mechanism associated with PI-modified CE and reported that crack bridging and crack pinning are the major toughening mechanisms. Kim et al.[109] evaluated toughening of CEs with PEI and concluded that co-continuous morphology causes toughening through crack deflection and crack pinning by PEI continuous domains, shown in Figure 14a, whereas in the phase-inverted morphology region, shown in Figure 14b, PEI matrix deformation is the major reason for the toughening.

Oyanguren et al.[67] examined the fracture toughening mechanism in the co-continuous morphology developed in a PSF-epoxy blend. They reported that in thermoplastic-rich domains, toughening mechanisms are the crack-path deflection, bifurcation lines, and plastic drawing of PSF-rich particles, while in thermoset-rich domains, plastic drawing of the PSF-rich phase along with stress whitening and debonding of thermoset-rich particles lead to toughening. Kinloch et al.[69] used the fracture mechanics approach to explain the effect of thermoplastic modification and mechanisms of toughening in modified CE systems. Polyester copolymer and hydroxyl-terminated PES

DOI: 10.1021/acs.iecr.7b05202
Ind. Eng. Chem. Res. 2018, 57, 4479−4504

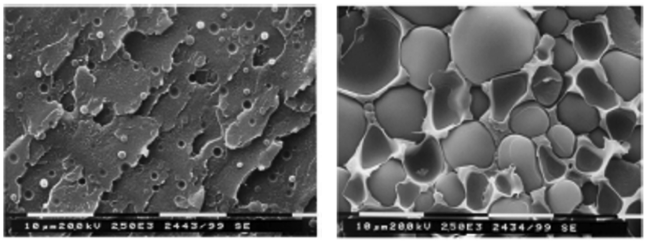

(a) (b)

Figure 14. Scanning electron micrographs: (a) co-continuous region and (b) phase-inverted region. Reprinted with permission from ref 109. Copyright 2002 Springer Nature.

were used to modify and improve the toughness of the CE resin. Tapered double cantilever beam (TDCB) testing was used to calculate fracture energies of the modified systems. For an unmodified system, stick/slip crack propagation was observed as a failure mechanism, which is associated with very brittle materials.[27] Figure 15 shows the SEM image of

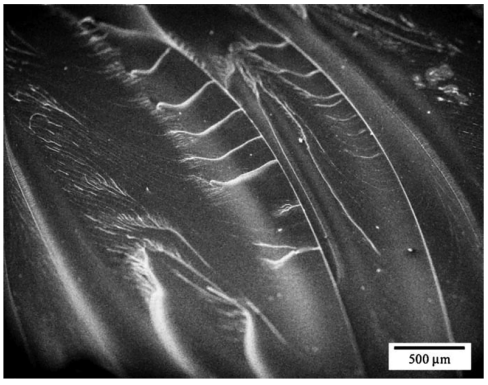

Figure 15. Scanning electron micrograph of unmodified BADCy resin. Reprinted with permission from ref 69. Copyright 2003 Springer Nature.

unmodified CE, in which the fracture surface is very glossy, indicating that little plastic deformation has occurred. Also, the fracture surface has steps and changes in the level of cracks, which are associated with feather markings caused by the crack forking in the fast brittle fracture.

For a PES/BADCy-modified system, phase-inverted morphology was observed for 20 wt% PES, and it was found that particles are not well bound with the matrix, as the surface of the particles was smooth, with no matrix material attached, as shown in Figure 16. Thus, the researchers concluded that cavitation and the plastic hole growth micro-mechanism are the toughening mechanisms for the modified system, which leads to a significant increase in fracture toughness.[69]

When cyanate resin based on phenolic triazine (PT) was modified with PES, the developed morphology showed a good adhesion between CE particles and PES matrix, thus failing by ductile tearing of matrix. Figure 17 shows the SEM image of PT resin modified with 10 wt% PES, showing good adhesion between particles and matrix phase.

Harismendy et al.[45] studied PEI toughening of CEs and concluded that particulate morphology corresponding to 10 wt % PEI led to toughening by crack path deflection and crack bridging with very little deboning present. They observed good adhesion between particles of the PEI and CE matrix.

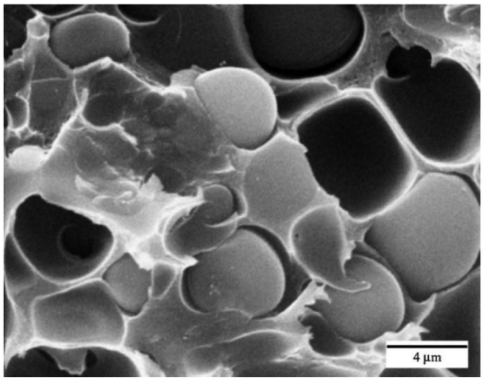

Figure 16. Scanning electron micrograph of 20 wt% PES/BADCy blend. Reprinted with permission from ref 69. Copyright 2003 Springer Nature.

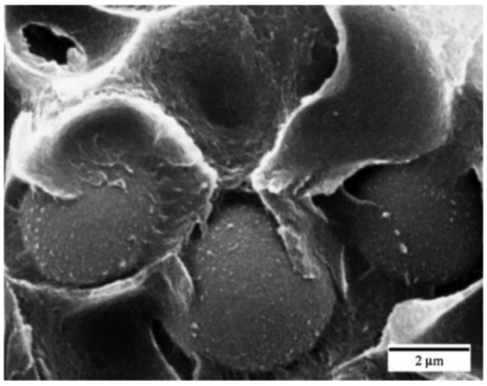

Figure 17. Scanning electron micrograph of 10 wt% PES/PT blend. Reprinted with permission from ref 69. Copyright 2003 Springer Nature.

8. STRUCTURE/PROPERTY RELATIONSHIP

The resulting properties of the blends are directly linked to the morphology obtained after phase separation. As per the discussions on the morphology and toughening mechanism, it can be concluded that co-continuous and phase-inverted morphologies are effective in toughness enhancement, and a higher degree of phase separation will lead to a higher toughening effect.[81] In the phase-inverted morphology, having good bonding between the phase-separated particle and matrix, plastic deformation of thermoplastic matrix is the mechanism which leads to significant toughening. In contrast, for the morphology with loosely bonded particles, toughness is enhanced via cavitation, plastic hole growth, and shear banding mechanism. Toughening in particulate morphology containing thermoplastic particles dispersed in the matrix follows the crack bridging mechanism along with crack pinning and crack deflection mechanisms. However, very fine particles dispersed in the matrix are ineffective and do not improve toughness significantly.[43,45] In the co-continuous morphology, plastic deformation of the thermoplastic-rich domain is the important mechanism which improves the toughness significantly. Functionalized thermoplastic such as cyanate-terminated PES result in blurring the interface in the morphology due to excellent bonding between the thermoplastic phase and matrix, further enhancing the toughness.[30] Thus, to enhance the toughness property of brittle CEs, co-continuous and phase-inverted morphologies are important along with use of functionalized thermoplastics.

DOI: 10.1021/acs.iecr.7b05202
Ind. Eng. Chem. Res. 2018, 57, 4479−4504

9. EXPERIMENTAL METHOD FOR THE MECHANICAL CHARACTERIZATION OF TOUGHENED BLENDS

Among all the properties, mechanical properties are usually the most important, as essentially all end applications and service conditions require some degree of mechanical loading. Selection of material for the application is often based on its mechanical properties such as fracture toughness, tensile strength, modulus, elongation, and impact strength. Hence, accurate characterization of these mechanical properties has become essential for successful design of the component. Thus, in this section, methods for characterizing the toughness and deformation of CEs and their thermoplastic blends are discussed in detail.

9.1. Fracture Toughness. A fracture mechanics approach is used to calculate the resistance of a material to the propagation of a present crack, called fracture toughness. This is an important property of a material and must be considered while designing the components for various applications. The fracture mechanics approach considers that the crack is present in the material at which stress concentration occurs during loading. The crack will then grow when the stress intensity at the crack tip exceeds the cohesive strength of the material.[110] It considers the linear elastic fracture mechanics in which all energy dissipation is due to the fracture process and the deformation that occurs is linear elastic. Fracture toughness of polymer/polymer blends is mainly characterized by single-edge-notch bending (SENB) and compact tension (CT) tests. ASTM D5045 is the most preferred standard method for these tests, which gives toughness in terms of the critical stress intensity factor (K_{IC}) and critical strain energy release rate (G_{IC}). In this method, pre-cracked specimen is loaded either in tension or in three-point bending, and the K_{IC} value is calculated from an equation which is derived from plane strain condition at the crack tip. A sharp notch is first machined in the sample and a crack is initiated by inserting a fresh razor blade at the notch and tapping the blade. The recommended initiated crack length for test is at least 2 times longer than the radius of the machined notch.

9.1.1. Single-Edge Notch Bending (SENB) Test. In this test, the specimen consists of a center notch and is loaded in three-point bending, as shown in Figure 18. For a specimen having

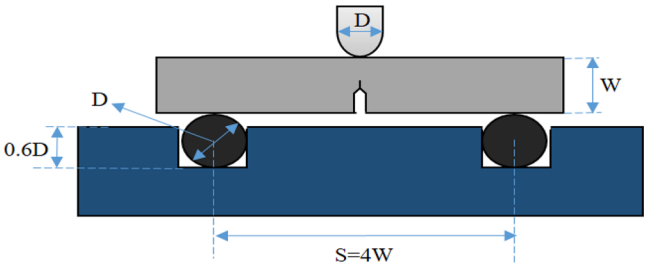

Figure 18. Single-edge notch bending test (SENB).

sheet geometry, sample thickness (B) should be assumed equal to sheet thickness, and width is taken as $W = 2B$. Initial crack length should be calculated such that $0.45 < a/W < 0.55$ (crack length nominally equal to thickness B and $W/B = 2$), which includes crack pre-notch plus razor notch. Specifications of a sample for the SENB test are shown in Figure 19. During the test, readings of load and corresponding displacement of crack are recorded to obtain a curve of load vs crack displacement.

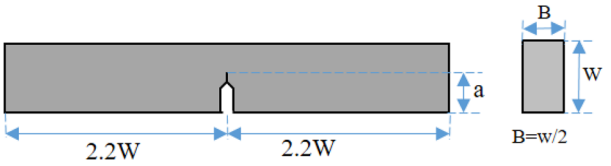

Figure 19. Test specimen for SENB test.

9.1.2. SENB Calculation of Fracture Toughness. Stress intensity factor K_{IC} is calculated using the following standard formula:

$$K_Q = \frac{P_Q}{BW^{1/2}} f(x), \quad \text{MPa·m}^{1/2} \tag{10}$$

where P_Q is the load (in kN), B is the specimen thickness (in cm), W is the specimen depth (in cm), a is the crack length (in cm), and $x = a/W$. For $0 < x < 1$,

$$f(x) = 6x^{1/2}\frac{[1.99 - x(1-x)(2.15 - 3.93x + 2.7x^2]}{(1+2x)(1-x)^{3/2}} \tag{11}$$

Strain energy release rate is given by a known relation,

$$G_{IC}\frac{(1-\nu^2)K_{IC}^2}{E} \tag{12}$$

where ν is Poisson's modulus and E is Young's modulus.

9.1.3. Compact Tension (CT) Test. The test specimen used in the CT test is shown in Figure 20, which considers

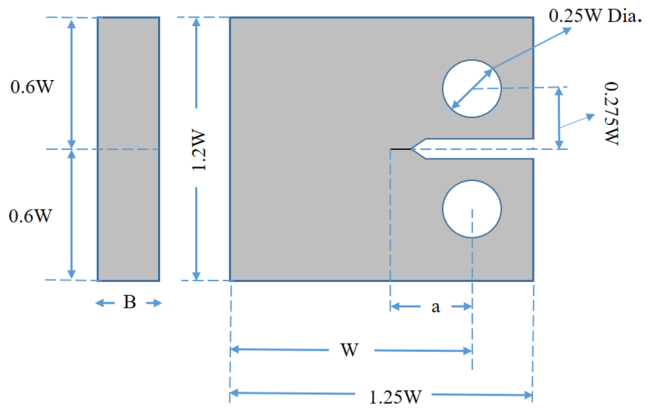

Figure 20. Test specimen for compact tension (CT).

dimensions such that the crack length (pre-notch plus razor notch) is $a = B$ and $W/B = 2$. Sample is loaded in tension on the machine which has a controlled constant displacement rate (e.g., Servo hydraulic Instron testing machine) using a fixture called clevis, and displacement of crack and corresponding load is recorded. Recommended cross heat rate is 10 mm/min for both test methods. During test, readings of load and corresponding displacement are recorded, and a curve of load vs displacement can be obtained.

9.1.4. CT Calculation of Fracture Toughness. Stress intensity factor (K_{IC}) is calculated using the following standard formula:

$$K_Q = \frac{P_Q}{BW^{1/2}} f(x) \tag{13}$$

DOI: 10.1021/acs.iecr.7b05202
Ind. Eng. Chem. Res. 2018, 57, 4479−4504

where P_Q is the load (in KN), B is the specimen thickness (in cm), W is the specimen depth (in cm), a is the crack length (in cm), and $x = a/W$. For $0.2 < x < 0.8$,

$$f(x) = \frac{(2 + x)(0.886 + 4.64x - 13.32x^2 + 14.72x^3 - 5.6x^4)}{(1 - x)^{3/2}} \quad (14)$$

Further, strain energy release rate is calculated using eq 12.

Various studies on thermoplastic-toughened resins have employed the above test methods for evaluation of fracture properties.[62,109,111−113] Yoon et al.[114] reported a SENB test with three-point bending mode at the rate of 0.5 in./min for PSF-toughened epoxy. In another study, Brooker et al.[115] reported a CT test for a thermoplastic-modified epoxy system. Samples with dimensions of 20 mm × 20 mm × 3.5 mm were used, and pre-cracked was done using a small hacksaw together with a razor blade to cut a sharp crack while loading at rate of 1 mm/min.

9.2. Tensile Properties. In a broad sense, tensile test is the measurement of a material's ability to withstand pulling force and quantifies the maximum deformation in the material before breaking. Tensile elongation and modulus are the most important parameters indicating strength of a material and are widely specified for a material. Tensile modulus, determined from a stress−strain diagram, gives information about the relative stiffness of a material, which is useful in designing components for a specific application. For the evaluation of tensile properties, a tensile testing machine with constant cross head movement is used, which has a one movable grip and one stationary grip with self-aligning ability, thereby preventing alignment problems. An extension indicator known as an extensometer is used to determine the relative distance between two designated points located along the gauge length during elongation of the test specimen. The specimen for tensile test can be prepared by either injection molding or compression molding for plastics.[116] Specimen may also be prepared by machining from a plate, slab or similar form. For CE blends, the process employed is to cast the film/cured resin in the mold followed by machining. Test specimen dimensions required for testing are described in detail in ASTM D638, which is the most commonly used standard for the measurement of tensile properties of plastics. This test uses a dumbbell-shaped specimen, and type I sample is mostly preferred for the test, as shown in Figure 21.

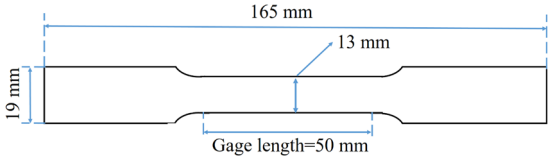

Figure 21. Test specimen of tensile test.

Five test speeds are specified in the standards; however, the most frequently used speed for the test is 0.2 in./min. To evaluate the tensile properties, test specimen is positioned on the grip of the machine and loaded at the rated speed. The load cell detects the resistance of the specimen to elongation, and the load values at yield, maximum, and break are recorded.

9.2.1. Calculation of Tensile Properties. A number of parameters such as tensile strength, percentage elongation at yield/break, modulus of elasticity, etc. can be calculated through tensile testing using the formulas given below:

$$\text{tensile strength} = \frac{\text{load (N)}}{\text{cross-section area (m}^2\text{)}}$$

$$\text{tensile strength at yield (MPa)} = \frac{\text{maximum load recorded (N)}}{\text{cross-section area (m}^2\text{)}}$$

$$\text{tensile strength at break (MPa)} = \frac{\text{load recorded at break (N)}}{\text{cross-section area (m}^2\text{)}}$$

Modulus and elongation properties are calculated from a stress−strain curve, for which an extensometer is attached to the specimen, which magnifies the actual elongation of the specimen. To calculate the modulus, a tangent is drawn to first linear straight portion of the curve, and two points are selected on the tangent as per convenience for recording stress and strain values. The formulas used to calculate modulus are as follow:

$$\text{tensile modulus (MPa)} = \frac{\text{difference in stress (N/m}^2\text{)}}{\text{difference in strain (m/m)}}$$

$$\text{tensile strain} = \frac{\text{change in length}}{\text{gauge length}}$$

Various studies on the thermoplastic-toughened blends of CEs also have reported tensile characterization. Tao et al.[71] and Zhan et al.[31] evaluated tensile properties of PEI- and PES-modified CE blends, respectively, using an Instron tensile tester with sample having gauge length of 15 mm and cross head speed of 1 mm/min. In another study, Srinivasan et al.[81] reported tensile properties for poly(arylene ether)-modified CE resin with a cross head speed of 1.27 mm/min.

9.3. Impact Properties. Impact resistance of a material is the ability of any material to resist fracture under high-speed stress loading. The impact properties are a measure of the overall toughness of a material, which is its ability to absorb energy before fracture. Impact strengths of polymeric materials are direct representations of their toughness characteristic, and the higher the impact strength, the higher will be the toughness. Impact properties of polymeric materials are usually calculated using the Izod−charpy impact test, as per ASTM standard D256. The objective of the Izod−charpy impact test is to calculate the strength of a standard test specimen to the pendulum impact load, and the results are expressed in terms of kinetic energy loss by the pendulum for the breaking of specimen. The energy absorbed in the breaking of specimen consists of the energy needed for the deformation of the specimen, to initiate a crack, to propagate the crack, and to toss the broken end of the specimen. Specimens used in the Izod test are notched to provide stress concentration, which promotes brittle fracture and thus prevents plastic deformation. In the Izod test, specimen is clamped vertically as a cantilever beam and it is struck by a swinging pendulum, released from a predetermined height over the specimen clamp. In the charpy test, a similar setup is employed, except here the sample is supported horizontally like a beam and fractured by a blow from the pendulum in the middle of the specimen. The dimensions of the sample used in Izod−charpy tests is as shown

DOI: 10.1021/acs.iecr.7b05202
Ind. Eng. Chem. Res. 2018, 57, 4479−4504

in Figure 22. The sample can be prepared either by molding or cutting from a sheet. The preferred width of the specimen is

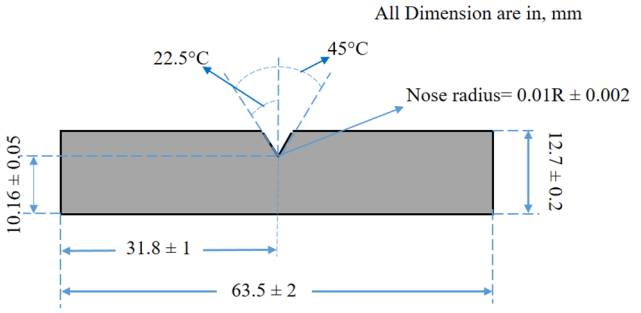

Figure 22. Izod−charpy impact test specimen.

6.35 mm or above, as test specimen having width less than this may overestimate the strength due to absorbed energy in crushing, bending, and twisting.

9.3.1. Izod Test. The clamping setup for the Izod test is shown in Figure 23, in which notch end is facing toward the

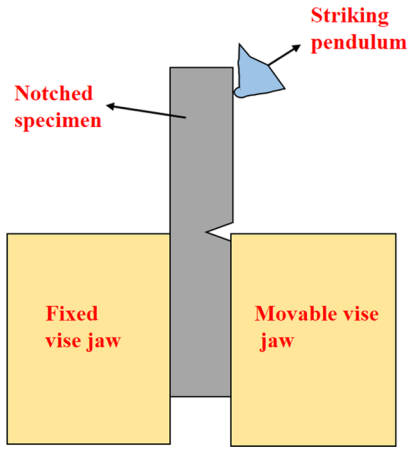

Figure 23. Schematic representation of Izod test.

strike edge of the pendulum. During the test, a pendulum with known mass is released from a pre-determined height, having a certain known potential energy, and allowed to strike the specimen. During the impact, energy absorbed in the fracture of specimen is read directly in units of in.-lbf or ft.-lbf from the scale or digital display. Impact strength is then calculated by dividing the energy absorbed in breaking by the thickness of the specimen.

9.3.2. Charpy Test. This test is similar to the Izod test, except for the sample positioning, as shown in Figure 24. Here

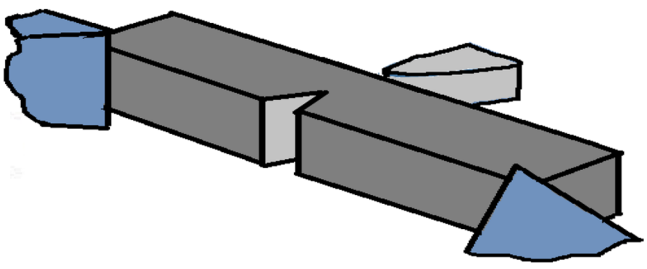

Figure 24. Schematic representation of Charpy test.

the sample is mounted horizontally and supported unclamped at both ends. Readings are taken for sample when the ends break completely, and impact strength is calculated by dividing the breaking energy by the thickness of the specimen.

9.4. Dynamic Mechanical Thermal Analysis (DMTA). DMTA is an advanced characterization technique to evaluate the viscoelastic properties of polymeric materials. In this technique, viscoelastic properties are measured in an oscillatory mechanical deformation experiment, as a function of temperature and frequency.[38,117] The DMTA analyzer consists of a linear drive motor to load the sample via probe, a sensor to measure displacement such as a linear variable differential transformer (LVDT), a temperature control furnace, a drive shaft, and clamps to hold the sample while testing. Based on the service condition of polymer blends, various deformation modes such as tension and compression, torsion and bending (single cantilever, dual cantilever, or three-point bending), and shear mode are employed in the characterization.[117]

DMTA works on the principle that when a polymer is subjected to external stimuli (e.g., mechanical), processes develop in its structure, such as changes in length and angle of bonds, which take time to bring into a new equilibrium. These processes in the structure functions of time called "relaxation time", which also depend upon temperature. During the recovery in the polymer, back-stress is created in the material opposite to applied stress, which causes a material to return to its original state when the external stress is removed. These stress levels are in the linear elastic range of a material, such that stress $\propto$ strain, and the proportionality constant is called Young's modulus (E). The analyzer gives thermograms as plots of elastic modulus, E and tan δ, versus temperature/frequency, from which viscoelastic properties of the material are recorded. The tan δ is the ratio of loss modulus (E'') to the storage modulus (E'), and its peak represents the T_g of the polymer. Storage modulus represents the energy absorbed and released elastically during deformation, while loss modulus represents the amount of energy absorbed by the material due to internal motions.

In DMTA experiment, the applied sinusoidal stress σ is such that the viscoelastic material loads in the elastic region. The expressions for the resultant sinusoidal stress and strain are as follow:

$$\sigma(t) = \sigma_0 \cos(i\,(\omega t)) \tag{15}$$

$$\varepsilon(t) = \varepsilon_0 \cos(i(\omega t + \delta)) \tag{16}$$

where ω is the angular frequency of the oscillation.

The equation for complex modulus is then given by

$$E^* = \frac{\sigma(t)}{\varepsilon(t)} = E' + iE'' \tag{17}$$

and

$$\tan\delta = \frac{E''}{E'} \tag{18}$$

where E'' is the loss modulus and E' is the storage modulus.

Various studies on thermoplastic-toughened CE blends have also been reported, using DMTA as a characterization tool for the evaluation of viscoelastic properties of blends.[26,73,70,118] Kim et al.[109] characterized the blend of PEI/CE using the DMTA technique in a dual-cantilever bending mode. Samples of dimensions 35 × 10 × 2 mm were loaded at a fixed frequency of 1 Hz and heating rate of 2 °C/min over a

DOI: 10.1021/acs.iecr.7b05202
Ind. Eng. Chem. Res. 2018, 57, 4479−4504

temperature range of 50−350 °C. The effects of the various morphologies generated on the loss and storage modulus of the blend were evaluated. In another study, Harismendy et al.[43] evaluated the viscoelastic property of BADCy/PEI blend using a three-point bending arrangement with a 44 mm span, and the elastic modulus property of the blend was reported. Thus, DMTA analysis is a tool that provides an understanding of the complexity that appears due to time−temperature dependency on the modulus of polymeric viscoelastic materials.

10. PROCESSING CHARACTERISTICS OF THERMOPLASTIC/CYANATE ESTER BLENDS

Processing characteristics of developed toughened thermoplastic/CE blends and various fabrication techniques applicable to processing these materials for manufacturing the final components/structures, e.g., fiber-reinforced composites, fibers, films, etc., are critically discussed in the next sections.

10.1. Processing Characteristics. CEs and their blends are still new materials in the field of structural composites. Owing to their processing similarities with epoxy resin, processing of these material to develop fiber-reinforced composites and other structures is not a challenge. Epoxy resins have been widely explored, and various methods have been developed for fabrication of high-quality fiber-reinforced composites. Hence, these processing techniques developed for epoxy resin can easily be imported for CEs with or without little modification. Cyanate ester monomers are available in a large variety of forms such as solid (REX-371), liquid (AroCy l-10), and semi-solid (XU71787);[4] hence, they offer an advantage for processing. Another advantage with CE monomers is their storage stability. Uncatalyzed CE monomers can be stored for more than 6 months at room temperature and for even longer duration at lower temperature.[4] CEs are self-curing resins in which curing is triggered by the temperature, though to increase the rate of cross-linking, a curing catalyst can also be used. Popular catalysts for CEs are chelates of metal ions and carboxylate salts[119,120] with co-catalyst nonylphenol.[30,77,121] Low toxicity is one of the important characteristics of CEs which simplifies the processing.[4,46] However, CEs are highly exothermic, and this should be carefully considered while processing.

10.2. Composite Fabrication Methods for Cyanate Esters and Their Blends. All common method for fabrication of composite can be used for CEs and their blends due to their processing similarities with epoxy resin. This processing advantage of CE resin makes them attractive for various commercial applications. CE resin also possesses excellent tack and drape characteristics, which are required for composite fabrication and hence avoids use of any external adhesive.[4] Developed composite processing techniques such as resin transfer molding (RTM),[77,122,123] resin film infusion (RFI),[77] prepregs,[17,122,124] filament windings,[125−128] autoclave molding,[12,129,130] pultrusion,[131,132] etc. can be efficiently used for fabrication of fiber-reinforced composites with CE resin. In the following section, commonly used composite fabrication techniques for structural applications are described in detail.

10.2.1. Resin Transfer Molding (RTM). RTM is a common composite fabrication technique widely used for fabrication of structural composites. A schematic of the RTM process is shown in Figure 25. In this technique, fiber preform or dry fiber reinforcement are placed on the surface of the lower half mold, and then the upper mold is closed.

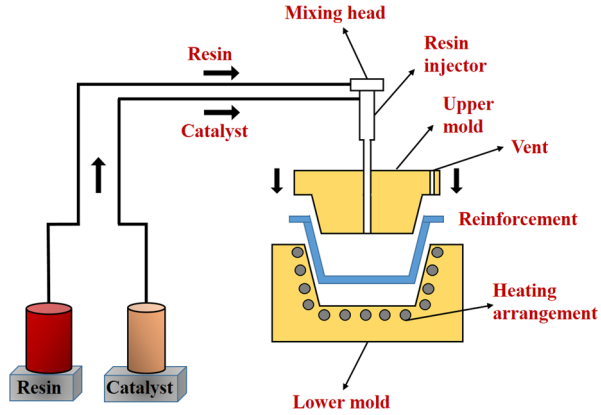

Figure 25. Schematic of resin transfer molding (RTM).

The mold has the shape of the desired part, and a release gel is applied on the mold surface for easy removal of the composite. Resin is then pumped into the mold under pressure, displacing the air through vents, until the mold is filled. The uniformity of resin flow can be enhanced by vacuum application.[21] After the fill cycle, the cure cycle starts, during which the mold is heated, and the resin polymerizes to become a rigid plastic, thus forming a composite.

The viscosity of the resin plays an important role in the RTM process because injection time depends upon viscosity of the resin. If viscosity of resin is high, high pressure is required, which may cause displacement of fibers inside the mold during the resin injection stage, known as fiber wash.[133] Recommended viscosity of resin for RTM is in the range of 100−300 cP.[1] Rau et al.[77] worked on a RTM for thermoplastic-toughened CE blend. Various molecular weights and formulations of poly(arylene ether sulfone) were blended with CEs, and carbon-fiber-reinforced composite laminates were fabricated using the RTM process. RTM technique resulted in high-quality laminate with void content less than 2%. Improvements in damage tolerance were reported for thermoplastics-modified composites, studied using compression after impact (CAI) test. Mechanical properties of the composite are listed in Table 7, which shows that high loading of thermoplastic at same molecular weight (15 000 g/mol) resulted in higher fracture toughness and flexural modulus. Also, an increase in molecular weight to 20 000 g/mol at the same concentration resulted in improved mechanical properties.

Table 7. Mechanical Properties of Carbon-Fiber-Reinforced Composite

	molecular weight (g/mol)	concn (%)	flexural modulus (GPa)	fracture toughness, G_{1IC} (kJ/m^2)	ref
CE			3.55	2.5	77
poly(arylene ether sulfone)/CE blend	15 000	20	3.98	3.1	77
	15 000	25	4.08	3.8	77
	15 000	30	4.4	3.94	77
	20 000	20	4.02	3.5	77

Hillermeier et al.[123,134] reported use of the RTM technique for thermoplastic- and elastomeric-toughened cyanate resin. Two thermoplastic, PEI and PS, were blended with CEs at 10 wt%, and glass-fiber-reinforced laminates were evaluated for

DOI: 10.1021/acs.iecr.7b05202
Ind. Eng. Chem. Res. 2018, 57, 4479−4504

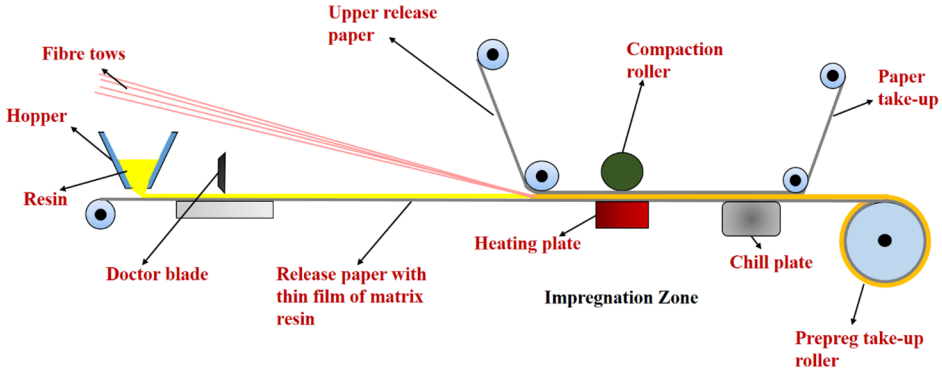

Figure 26. Schematic of hot-melt prepreg process.

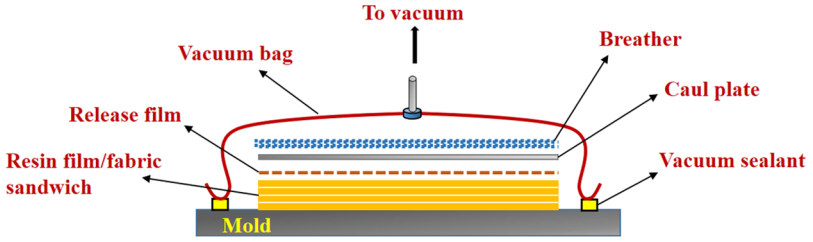

Figure 27. Schematic of resin film infusion (RFI) process.

their mechanical properties. Fracture toughness values of 653 and 563 J/m^2 were reported for PEI and PS matrices, respectively. Parlevliet et al.,[122] from the airbus group, investigated composite properties of epoxy/CE blends manufactured by RTM and showed excellent high-temperature stability of the product.

10.2.2. Prepreg and Autoclave Molding. The prepreg technique has been an attractive choice for CE composites in the past. Prepregs are the pre-impregnating fiber materials, which can be impregnated either in resin solution or in filming technique (hot melt process). A large variety of fibers such as carbon, aramid, glass, quartz, etc. can easily be prepregged.[4] In the solution technique, impregnation of reinforcement is achieved by dipping the fiber material in molten resin. In an alternate method, the hot melt process, films of resin and reinforcing fiber are sandwiched between two release films, with simultaneous application of heat and pressure,[135] as shown in Figure 26. Generally, fabrication of composites with stacks of prepregs is achieved by an autoclave or compression molding process.[126] In an autoclave, prepregs are stacked in a mold in a definite sequence and then spot-welded to avoid any relative movement in between the prepreg sheets. After stacking of the prepregs, the whole assembly is vacuum-bagged to remove any air entrapped in between the layers. The entire assembly is then transferred to an autoclave, which provides the heat and pressure required for consolidation and curing of resin. The prepreg technique has been widely explored for CEs, and a significant amount of literature is available. Wang et al.[124] reported a prepreg technique for fabrication of composite with PEI and polyamideimide-toughened cyanate resin. They reported that the resultant composite has a low heat release rate and self-extinguish time of only 4 s. Autoclave processing for composites was studied by Hayes et al.[130] for a glass-fiber-reinforced composite with an elastomer-toughened cyanate resin. Epoxy-terminated butadine acrylonitrile rubber was used to modify CE resin, which resulted in an increase in mode I fracture toughness by 2-fold as compared to unmodified CEs. However, water absorption was found to increase as a result of rubber modification. Barton et al.[12] investigated prepregging and autoclave technique for BMI/CE blends. Their study concluded that a blend of 50 wt% BMI and 50 wt% CE gives maximum interlaminar shear strength (109.7 MPa). Parlevliet et al.[122] investigated epoxy-modified CE composite fabricated using the prepreg process. The formulated blend possessed excellent track and drape, resulted in easy processing through prepreg and composite structure showed high stability and good mechanical properties at elevated temperature (135 °C). Mathew et al.[17] and Hamerton et al.[129] also investigated the prepreg technique for fiber-reinforced CE composites fabrication and concluded that prepreg and autoclave processes can be easily imported in these blends.

10.2.3. Resin Film Infusion (RFI). RFI is a liquid molding technique that is emerging as an alternative to RTM. It reduces the cost of tooling required to keep the quality of composites comparable to that achieved with RTM.[136] A schematic of the RFI technique for fabrication of composites is shown in Figure 27. In this technique, a sandwich of resin film and fiber cloths is formed by alternate layering of them in the required fashion, which is then vacuum-bagged as per the sequence shown in Figure 27. Peel ply is used for easy removal of composite and bleeder to absorb excess resin.[137] The entire bagged assembly is then heated to cure the resin while simultaneously maintaining the vacuum pressure for consolidation. Under heat, the viscosity of the resin film decreases, allowing resin to flow, and vacuum pressure causes consolidation and infusion of resin into the fiber, thus impregnating it.

High-viscosity cyanate resins are suitable for fabricating composite panels using the RFI process, as they possess film formability. Although it is an important technique for structural composites, literature on RFI studies on CEs is limited. Rau et al.[77] investigated RFI for CE/PSF blends and suggested that RFI is a suitable composite fabrication technique for high-viscosity resins. Poly(arylene ether sulfone) with molecular weight of 15 000 g/mol, when blended at a higher loading of 25

DOI: 10.1021/acs.iecr.7b05202
Ind. Eng. Chem. Res. 2018, 57, 4479−4504

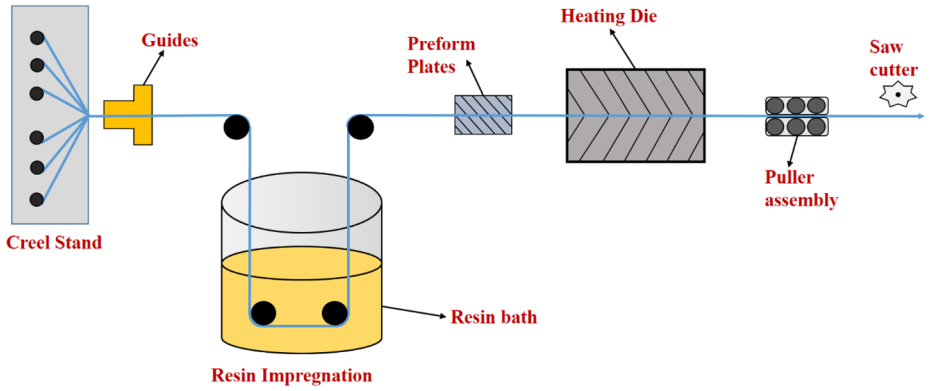

Figure 28. Schematic of pultrusion process.

wt%, resulted in an increase in viscosity; thus, the RFI process was used to fabricate composite samples. Mechanical properties of the composite are listed in Table 7. In the case of thermoplastic toughening, higher thermoplastic loading in CEs results in a significant increase in viscosity; thus, higher pressure is needed for fabrication of composites via RTM, which then increases the chance of fiber wash. However, this increased viscosity of resin is an advantage for RFI, as resin film can be easily cast.

10.2.4. Pultrusion. Pultrusion[138] is a continuous composite fabrication process in which composites are formed by pulling the reinforcement through a heated closed die of the required shape. A schematic representation of the pultrusion process is shown in Figure 28. Reinforcement in the form of either continuous rovings or fiber cloths is unrolled from the creel and passes through the resin tank, which saturates the fiber. The impregnated reinforcement is then guided to the hot die, where the reinforcement is shaped into the desired profile, while simultaneous curing the resin due to heating.[139] A built-in cutting mechanism then cuts the composite profile in the final shape. Some pultrusion systems also employ a pre-former to squeeze out excess polymer before passing to the hot die section. Thus, in the pultrusion process, a constant cross-section profile of the composite product is produced on a continuous basis. Shivakumar et al.[131,132] fabricated a CE composite rod with carbon fiber using the pultrusion technique and proposed its application for brush seals in gas turbine engines.

10.2.5. Filament Winding (FW). In the FW method, fiber strands are passed through resin tanks to impregnate the fiber completely. These impregnated fiber strands are then passed onto a rotating mandrel, where they get wound in a controlled manner and in a specific fiber orientation. Figure 29 shows a schematic of the FW process. In this process, fiber tension is the critical parameter, because compaction is achieved through the fiber tension. Optimum fiber tension is required so as to avoid porosity in the composite. At the same time, too high tension may break the fiber or initiate fiber fracture at the surface. Finally, curing of resin is done by heating in an oven, and the final composite product is taken out from the mandrel. For complex shapes, soluble plaster or collapsible rubber can be used for the mandrel. This method is widely used for making pipes, pressure vessels, tanks, etc. Cyanate esters (PT resin) have successfully undergone FW for cylindrical structures (e.g., pressure bottles) and showed excellent properties even at high temperature ($T \approx 288$ °C).[125] Esslinger et al.[126] manufactured filament wound CE composite structures for missile application, and improvement in thermal performance was reported. Tian et al.[127] studied the properties of carbon fiber laminate manufactured by a wet FW process with epoxy/CE resin. They reported that the formed laminate composite has a long service life characterized by the standard vessel explosion test. CE resins have also been used for FW of cylindrical structures and rings with carbon fibers.[125] Cui et al.[128] used the FW technique for epoxy and BMI-modified CE resin and reported that the formed composite had excellent strength and thermal stability. A comparison of all composite fabrication processes is illustrated in Table 8.

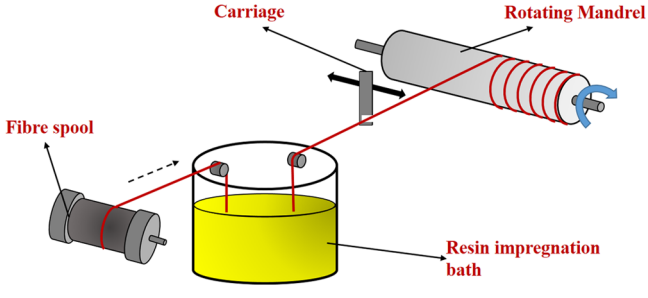

Figure 29. Schematic of filament winding (FW) process.

10.3. Processing of Fibers. Over the past few years, polymer nanofibers have been popular among researchers due to their wide applicability. They have been continuously studied for their use in filters, scaffolds, sensors, reinforcements in composite materials, protective clothing, etc.[140−149] Most thermosetting resins used in fiber-reinforced composites suffer from poor delamination, poor fracture strength, and poor impact resistance.[150] Recently, toughening of fiber reinforced composites with interleaved nanofibers veils has become popular, due to the selective improvement in properties without degrading other mechanical properties.[151−153] A large number of studies on enhancement of toughness with interleaved nanofibers have been reported for fiber-reinforced epoxy composites.[154−157] This approach can also be easily extended for CE-fiber-reinforced composites. Conventional techniques such as drawing, template synthesis, phase separation, self-assembly, and electrospinning have been used to form nanofibers. Due to its simplicity and higher efficiency, electrospinning is the most popular method used to form nanofibers. The drawback of low production volume of conventional electrospinning can be overcome by use of multi-needle electrospinning and needleless spinning, but at the expense of increase in production cost.[158] Other techniques,

DOI: 10.1021/acs.iecr.7b05202
Ind. Eng. Chem. Res. 2018, 57, 4479−4504

Table 8. Comparison of Composite Fabrication Techniques

fabrication technique	advantages	disadvantages
resin transfer molding	1. good surface finish on both sides of the product surface	1. mold cavity limits the size of the composite
	2. higher production rate	2. high tooling cost
	3. process can be manual control, semi-automated, or highly automated	3. matched tooling is expensive and heavy in order to withstand pressure
	4. uniform composite part thickness	4. generally limited to small size components
	5. low emission during composite processing	5. possibility of un-impregnated areas
	6. strict dimensional tolerances	
	7. high injection pressure is not required	
	8. low material waste due to near net shape parts fabrication	
autoclave molding	1. achieve high volume fraction of reinforcement	1. part size depends upon the autoclave size
	2. minimal void content in the finished part due to removing entrapped air through vacuum	2. high cost of production
	3. high degree of uniformity in part consolidation	3. low rate of production
	4. applicable for both thermoplastic and thermosetting polymer composites	
resin film infusion	1. high fiber volumes can be accurately achieved with low void contents	1. not widely proven outside the aerospace industry
	2. potentially lower cost than prepreg	2. an oven and vacuum-bagging system are required to cure the component, as for prepreg
	3. complex shaped parts can be manufactured with ease	
	4. local flow of resin ensures complete wetting of fibres	
	5. suitable for filler/functional composites	
pultrusion	1. low cost and automated process	1. suitable for constant cross-sectional areas
	2. produces high-quality parts	2. tapered and complex shapes cannot be produced
	3. high surface finish as compared to other composite processing methods	3. control of fiber orientation is not possible
	4. high rate of production, as it is a continuous production process	4. thin wall parts cannot be produced
	5. high fiber volume fraction in the parts	5. limited to constant or near-constant cross-section components
	6. resin content can be accurately controlled	6. heated die costs can be high
	7. resin impregnation area can be enclosed, thus limiting volatile emissions	
filament winding	1. high strength-to-weight ratio in fabricated parts	1. capital investment is relatively high
	2. high degree of uniformity in fiber distribution, orientation, and placement	2. very precise control over the mechanism is required for uniform distribution and orientation of fiber
	3. labor involvement is minimal, as it is an automated process	3. composite product configuration is such that it should facilitate in Mandrel extraction
	4. design flexibility possible with the change in winding patterns, material, and curing option	4. surface finish is poor
	5. size of the component is not restricted	5. fiber direction cannot be changed within one layer of winding
	6. high production volume	
	7. process automation results in cost saving	

such as centrifugal rotary spinning,[159,160] pressurized gyration,[161,162] force spinning,[163] and infusion gyration,[162] which utilizes centrifugal force to produce fibers, are gaining attraction over electrospinning, as they are largely independent of the materials' properties. Hong et al.[164] in their recent study reported the "pressure coupled infusion gyration" process as an effective alternative to electrospinning. This technique uses both pressure and centrifugal force to produce fibers. It consists of the central vessel on which orifices are mounted at equidistance, driven by a DC motor. Via syringe, polymer solution is infused into the bottom of the vessel, and high-pressure nitrogen gas is used to force the solution through the orifices. The researchers demonstrated the process and reported that 60−850 nm diameter fibers were produced with poly(ethylene oxide) polymer solution. The major advantage with this technique is that its yield efficiency is very high, along with low tooling cost.

11. APPLICATION OF CYANATE ESTER COMPOSITES

Enhanced mechanical properties of modified CE resins make them strong matrix materials for advanced structural composites. Properties of CEs like low moisture absorption,[156] high dimensional and thermal stability, excellent electrical properties, low flammability,[125] etc. make them favorable matrices in composites, over conventional epoxy resins and other high-temperature resins. High moisture absorption in any resin system has adverse effects on the performance of system, as it causes a change in dimension, reduces T_g, deteriorates the hot-wet performance of the system, and also causes micro-cracking.[46] Further, absorbed moisture causes an increase in dielectric constant of system, which then reduces the

DOI: 10.1021/acs.iecr.7b05202
Ind. Eng. Chem. Res. 2018, 57, 4479−4504

performance in applications such as radomes, radars, printed circuit boards, leading edges, etc. CEs absorb almost one-fourth the moisture absorbed by conventional epoxies.[4] Thus, the use of CEs in one of these applications has an advantage of low moisture absorption, overcoming the above listed problems and thus improving the performance of the system.[4] In the next section, we discuss various potential applications of CE resins and their composites, which includes applications in primary structural composites, aero-space structures, electronic equipment, satellite components, etc.

11.1. Primary Structural Applications. Applications which have significant load-bearing requirement and are flight critical are termed as primary structures.[157] In such applications, one of the major drawbacks of a conventional material like epoxy is its brittle nature and high moisture absorption. Cyanate esters are inherently tougher than epoxies, and thermoplastic-toughened CE blends result in phase separation, exhibiting highly improved toughness of resin.[48] Also, high-temperature performance of toughened system and solvent/chemical resistance are key advantages associated with the use of CEs for structural applications.[125] One of the major requirements of resin in structural applications is the balance between damage tolerance and hot-wet performance. Thus, thermoplastic-toughened CEs provide an excellent balance between toughness and compressive strength, without degrading creep- and solvent-resistance properties.[45,71] Such primary structural applications include parts around aero-engines, tail assembly, air ducts in aircrafts, muffler systems in high-speed racing cars, rotor blades in helicopters, etc.[64,125,158] In developing high-speed missiles, e.g., Mach 3, the temperature produced at the nose is high ($T \approx 500$ °C), and hence, high-T_g CEs toughened with thermoplastic composites out-perform ceramic materials, due to their high short-term thermal stability, light weight, and low production cost.[125]

11.2. Satellite/Space Application. Components used in satellite applications such as optical benches, reflectors, dimensionally stable platforms, etc. currently use high-modulus graphite/epoxy composites.[157] However, high moisture absorption of epoxy systems is the main drawback, which affects the performance of composites and makes them prone to microcracks when thermally cycled. Also, high outgassing of resin used in space applications is a major problem, as it can condense on optical and electronics components of the system, thereby reducing their performance. Hence, the low outgassing property of CEs is an another important advantage in satellite applications,[159,160] along with low moisture absorption and high-dimensional stability. CEs have <1% outgassing volatile loss and <0.1% condensable volatiles.[125] High T_g of CEs and excellent stability against radiation exposure are key advantages associated with the use of CEs in space applications.[160,161] Further, the use of lightweight composite structures instead of metal results in significant savings in launch cost in space applications.

11.3. Radomes and Radar Components. The low dielectric loss property of CEs makes them a suitable material in applications such as radomes, and other parts in radar systems.[160,162] Radomes used in military and commercial vehicles have been made with epoxy or polyester resins.[4] However, with increasing demand for radomes for applications at high frequencies (9−44 GHz),[160] the need for a material with a low dissipation factor and high T_g makes CEs a primary material of choice.[162,163] In such high-frequency applications, absorbed electrical signal causes heating of radomes; hence, high T_g is essential. Also, modified CEs result in an improved mechanical property, which fulfills the damage tolerance and load-bearing requirements in these applications. Low moisture absorption is again an advantage of the use of CE resins in radomes and radar components, as dielectric properties remain unaffected.

11.4. Radar-Absorbing Structures and Microwave Communication Systems. Over the past few years, radar-absorbing composite structures (RAS) have become popular in aero-structures due to their high strength-to-weight ratio. In these applications, low dielectric loss (D_k) is essential, and hence, CE resins with low D_k fibers (e.g., quartz) have been of interest in research. Use of these composites can lead to reduction in the radar cross-section, thereby increasing the range and maneuverability of aircrafts.[125] Also, CEs meet the thermal requirements essential for these applications and have adequate strength. Another important application of CE composites is to protect windows or antennae in microwave communication and tracking devices. These composites offer an advantage of reduced reflection of signals, thereby increasing the strength and quality of signals. Such applications include protection for communication systems in fuselages, leading edges, and nose of aircrafts. CEs have been primary choice of material in high-speed electronic systems such as printed circuit boards and already inducted in many such applications.[160,164,165]

12. CONCLUSION

This Review describes and gives examples of the mechanical attributes of thermoplastics-toughened cyanate esters in fiber-reinforced composites for structural applications. Thermoplastics blends have been reviewed for their phase-separation-induced morphologies and the various resulting toughening mechanisms involved. It has been observed that the viscosity of a blend defines the mechanism of phase separation; hence, monitoring of viscosity through control over molecular weight and concentration of thermoplastic allows one to tailor the morphology of a cured system. It has been elaborated that the toughness of high-temperature thermosetting CEs is significantly improved as a result of thermoplastic blending. The co-continuous and phase-inversion morphologies which are essential and decisive for toughness enhancement are generally observed at higher loadings of thermoplastics. In contrast to rubber blending, the high-temperature properties of elucidated thermoplastics blends are not altered. Processing of these blends is analogous to that of epoxy systems, and hence, composites fabrication techniques such as resin transfer molding, resin film infusion, autoclave, etc. can be advocated for CE blends with minor alteration, which has also been discussed in the current Review. Applications of modified CE matrix/fiber-reinforced composites have also been exploited and discussed in detail, including applications in radomes and radar components, primary structures, satellites, radar absorbing structures, etc., where high temperature is a critical aspect. Thus, we envision that thermoplastics-toughened CE-based composites have wide applicability as materials of the future where high service temperatures are essential.

AUTHOR INFORMATION

Corresponding Author

*Tel.: 91-20-24304207. Fax: +91-20-24388835. E-mail: meetkbs@gmail.com.

DOI: 10.1021/acs.iecr.7b05202
Ind. Eng. Chem. Res. 2018, 57, 4479−4504

ORCID

Balasubramanian Kandasubramanian: 0000-0003-4257-8807

Notes

The authors declare no competing financial interest.

■ ACKNOWLEDGMENTS

The authors would like to thank Dr. Surendra Pal, Vice Chancellor, Defence Institute of Advanced Technology (DU), Pune, for support. The authors also acknowledge Mr. Ramdayal Yadav and Mr. Prakash Gore for their continuous technical support during the preparation of the manuscript.

■ REFERENCES

(1) King, J. A.; Klimek, D. R.; Miskioglu, I.; Odegard, G. M. Mechanical properties of graphene nanoplatelet/epoxy composites. *J. Compos. Mater.* **2015**, *49*, 659−668.

(2) Toldy, A.; Szolnoki, B.; Marosi, G. Flame Retardancy of Fibre-Reinforced Epoxy Resin Composites for Aerospace Applications. *Polym. Degrad. Stab.* **2011**, *96*, 371−376.

(3) Browning, C. E. The Mechanisms of Elevated Temperature Property Losses in High Performance Structural Epoxy Resin Matrix Materials after Exposures to High Humidity Environments. *Polym. Eng. Sci.* **1978**, *18*, 16−24.

(4) Hamerton, I. *Chemistry and Technology of Cyanate Ester Resins*; Springer: Dordrecht, 1994.

(5) Ju, J.; Morgan, R. J. Characterization of microcrack development in BMI-carbon fiber composite under stress and thermal cycling. *J. Compos. Mater.* **2004**, *38*, 2007−24.

(6) Morgan, R. J.; Jurek, R. J.; Yen, A.; Donnellan, T. Toughening Procedures, Processing and Performance of Bismaleimide-Carbon Fibre Composites. *Polymer* **1993**, *34*, 835−842.

(7) Meador, M. A. Recent Advances in the Development of Processable High-Temperature Polymers. *Annu. Rev. Mater. Sci.* **1998**, *28*, 599−630.

(8) Mittal, K. L. *Polyimides and other high temperature polymers: synthesis, characterization and applications*; CRC Press: Boca Raton, FL, 2005; Vol. 3.

(9) Hamerton, I.; Hay, J. N. Recent technological developments in cyanate ester resins. *High Perform. Polym.* **1998**, *10*, 163−174.

(10) Wooster, T. J.; Abrol, S.; Hey, J. M.; MacFarlane, D. R. Thermal, Mechanical, and Conductivity Properties of Cyanate Ester Composites. *Composites, Part A* **2004**, *35*, 75−82.

(11) Shen, Y.; Gu, A.; Liang, G.; Yuan, L. High Performance CaCu3Ti4O12/cyanate Ester Composites with Excellent Dielectric Properties and Thermal Resistance. *Composites, Part A* **2010**, *41*, 1668−1676.

(12) Barton, J. M.; Hamerton, I.; Jones, J. R.; Stedman, J. C. Mechanical Properties of Tough, High Temperature Carbon Fibre Composites from Novel Functionalized Aryl Cyanate Ester Polymers. *Polymer* **1996**, *37*, 4519−4528.

(13) Shimp, D. A.; Christenson, J. R.; Ising, S. J. *Proc. Int. SAMPE Symp. Exhibition* **1989**, *34*, 222.

(14) Ng, L. H.; Field, F. R., III. Materials for printed circuit boards: Past usage and future prospects. *Materials and Society (United States)* **1989**, 13.

(15) Shimp, D. A. Technologically driven applications for cyanate ester resins. *Chemistry and technology of cyanate ester resins*; Springer: Dordrecht, 1994; pp 282−327.

(16) Boyd, J. D.; Sitt, H.; Ryang, H.; Biermann, T. F. Structures exhibiting improved transmission of ultrahigh frequency electromagnetic radiation and structural materials which allow their construction. U.S. Patent 4,956,393, 1990.

(17) Mathew, D.; Nair, C. P. R.; Ninan, K. N. Bisphenol A Dicyanate−Novolac Epoxy Blend: Cure Characteristics, Physical and Mechanical Properties, and Application in Composites. *J. Appl. Polym. Sci.* **1999**, *74*, 1675−1685.

(18) Jayakumari, L. S.; Thulasiraman, V.; Sarojadevi, M. Synthesis and characterization of cyanate epoxy composites. *High Perform. Polym.* **2007**, *19*, 33−47.

(19) Ganesan, A.; Muthusamy, S. Mechanical properties of high temperature cyanate ester/BMI blend composites. *Polym. Compos.* **2009**, *30*, 782−790.

(20) Ren, P.; Liang, G.; Zhang, Z. Epoxy-modified cyanate ester resin and its high-modulus carbon-fiber composites. *Polym. Compos.* **2006**, *27*, 402−409.

(21) Nair, C. P. R.; Francis, T.; Vijayan, T. M.; Krishnan, K. Sequential Interpenetrating Polymer Networks from Bisphenol A Based Cyanate Ester and Bimaleimide: Properties of the Neat Resin and Composites. *J. Appl. Polym. Sci.* **1999**, *74*, 2737−2746.

(22) Gu, A. High Performance Bismaleimide/cyanate Ester Hybrid Polymer Networks with Excellent Dielectric Properties. *Compos. Sci. Technol.* **2006**, *66*, 1749−1755.

(23) Feng, Y.; Fang, Z. P.; Gu, A. Toughening of Cyanate Ester Resin by Carboxyl Terminated Nitrile Rubber. *Polym. Adv. Technol.* **2004**, *15*, 628−631.

(24) Shi, H.; Fang, Z.; Gu, A.; Tong, L.; Xu, Z. Carboxyl-terminated butadiene−acrylonitrile rubber modified cyanate ester resin. *J. Appl. Polym. Sci.* **2007**, *106*, 3098−3104.

(25) Pascault, J. Rubber- and thermoplastic-modified polymer networks. Phase separation process induced by polymerization and polycondensation. *Macromol. Symp.* **1995**, *93*, 43−51.

(26) Thunga, M.; Akinc, M.; Kessler, M. R. Tailoring the Toughness and CTE of High Temperature Bisphenol E Cyanate Ester (BECy) Resin. *eXPRESS Polym. Lett.* **2014**, *8*, 336−344.

(27) DiBerardino, M. Toughening mechanisms in a high temperature cyanate ester resin modified with a thermoplastic polyimide. Ph.D. Thesis, Lehigh University, 1993.

(28) Kim, Y. S.; Min, H. S.; Kim, S. C. Polyetherimide/dicyanate semi-interpenetrating polymer networks having a morphology spectrum. *Macromol. Res.* **2002**, *10*, 60−66.

(29) Hwang, J. W.; Cho, K.; Park, C. E.; Huh, W. Phase Separation Behavior of Cyanate Ester Resin/polysulfone Blends. *J. Appl. Polym. Sci.* **1999**, *74*, 33−45.

(30) Chang, J. Y.; Hong, J. L. Morphology and Fracture Toughness of Poly (Ether Sulfone)-Blended Polycyanurates. *Polymer* **2000**, *41*, 4513−4521.

(31) Zhan, G.; Hu, S.; Yu, Y.; Li, S.; Tang, X. The study on poly (ether sulfone) modified cyanate ester resin and epoxy resin cocuring blends. *J. Appl. Polym. Sci.* **2009**, *113*, 60−70.

(32) Wang, G.; Wang, R.; Fu, G.; Gao, T.; Fu, C.; Kuang, H.; Yang, F.; Jiao, W.; Hao, L.; Liu, W. Study on phenolphthalein poly (ether sulfone)-modified cyanate ester resin and epoxy resin blends. *Polym. Eng. Sci.* **2015**, *55*, 2591−2602.

(33) Utracki, L. A.; Wilkie, C. A. *Polymer blends handbook*; Kluwer Academic Publishers: Dordrecht, 2002; Vol. 1.

(34) Wertz, D. H.; Prevorsek, D. C. Dicyanate Semi IPNs-A New Class of High Performance, High Temperature Plastics. *Polym. Eng. Sci.* **1985**, *25*, 804−806.

(35) Dobry, A.; Boyer-Kawenoki, F. Phase Separation in Polymer Solution. *J. Polym. Sci.* **1947**, *2*, 90−100.

(36) Voorn, M. J. Phase separation in polymer solutions. *Forschritte Der Hochpolymeren-Forschung*; Springer: Berlin/Heidelberg, 1959; pp 192−233.

(37) Flory, P. J. *Principles of Polymer Chemistry*; Cornell University Press: New York, 1953.

(38) Thomas, S.; Grohens, Y.; Jyotishkumar, P. *Characterization of polymer blends: miscibility, morphology and interfaces*; John Wiley & Sons: New York, 2014.

(39) Zhan, G.; Yu, Y.; Tang, X.; Tao, Q.; Li, S. Further Study of the Viscoelastic Phase Separation of Cyanate Ester Modified with Poly(ether Imide). *J. Polym. Sci., Part B: Polym. Phys.* **2006**, *44*, 517−523.

(40) Borrajo, J.; Riccardi, C. C.; Williams, R. J. J.; Cao, Z. Q.; Pascault, J. P. Rubber-Modified Cyanate Esters: Thermodynamic Analysis of Phase Separation. *Polymer* **1995**, *36*, 3541−3547.

DOI: 10.1021/acs.iecr.7b05202
Ind. Eng. Chem. Res. 2018, 57, 4479−4504

(41) Iijima, T.; Katsurayama, S.; Fukuda, W.; Tomoi, M. Modification of cyanate ester resin by poly (ethylene phthalate) and related copolyesters. *J. Appl. Polym. Sci.* **2000**, *76*, 208−219.
(42) Sperling, L. H. Interpenetrating Polymer Networks: An Overview. *Adv. Chem. Ser.* **1994**, *239*, 3−38.
(43) Harismendy, I.; Del Río, M.; Eceiza, A.; Gavaldá, J.; Gómez, C. M.; Mondragon, I. Morphology and Thermal Behavior of Dicyanate Ester-Polyetherimide Semi-IPNS Cured at Different Conditions. *J. Appl. Polym. Sci.* **2000**, *76*, 1037−1047.
(44) Fay, J. J.; Murphy, C. J.; Thomas, D. A.; Sperling, L. H. Effect of Morphology, Crosslink Density, and Miscibility on Interpenetrating Polymer Network Damping Effectiveness. *Polym. Eng. Sci.* **1991**, *31*, 1731−1741.
(45) Harismendy, I.; Del Rio, M.; Marieta, C.; Gavalda, J.; Mondragon, I. Dicyanate Ester−Polyetherimide Semi-Interpenetrating Polymer Networks. II. Effects of Morphology on the fracture toughness and mechanical properties. *J. Appl. Polym. Sci.* **2001**, *80*, 2759−2767.
(46) Fang, T.; Shimp, D. A. Polycyanate Esters: Science and Applications. *Prog. Polym. Sci.* **1995**, *20*, 61−118.
(47) Zhou, C.; Gu, A.; Liang, G.; Yuan, L. Novel Toughened Cyanate Ester Resin with Good Dielectric Properties and Thermal Stability by Copolymerizing with Hyperbranched Polysiloxane and Epoxy Resin. *Polym. Adv. Technol.* **2011**, *22*, 710−717.
(48) Hwang, J. W.; Park, S. D.; Cho, K.; Kim, J. K.; Park, C. E.; Oh, T. S. Toughening of Cyanate Ester Resins with Cyanated Polysulfones. *Polymer* **1997**, *38*, 1835−1843.
(49) Kinloch, A. J.; Hunston, D. L. Effect of Volume Fraction of Dispersed Rubbery Phase on the Toughness of Rubber-Toughened Epoxy Polymers. *J. Mater. Sci. Lett.* **1987**, *6*, 137−139.
(50) Ratna, D.; Banthia, A. K. Rubber toughened epoxy. *Macromol. Res.* **2004**, *12*, 11−21.
(51) Kinloch, A. J.; Shaw, S. J.; Tod, D. A.; Hunston, D. L. Deformation and Fracture Behaviour of a Rubber-Toughened Epoxy: 1. Microstructure and Fracture Studies. *Polymer* **1983**, *24*, 1341−1354.
(52) Thomas, R.; Yumei, D.; Yuelong, H.; Le, Y.; Moldenaers, P.; Weimin, Y.; Czigany, T.; Thomas, S. Miscibility, Morphology, Thermal, and Mechanical Properties of a DGEBA Based Epoxy Resin Toughened with a Liquid Rubber. *Polymer* **2008**, *49*, 278−294.
(53) Bucknall, C. B.; Yoshii, T. Relationship between structure and mechanical properties in rubber-toughened epoxy resins. *Br. Polym. J.* **1978**, *10*, 53−59.
(54) Luxia, L. Y. Study on toughening Bismaleimide with CTBN rubber. *New Chem. Mater.* **2001**, *2*, 007.
(55) Shaw, S. J.; Kinloch, A. J. Toughened Bismaleimide Adhesives. *Int. J. Adhes. Adhes.* **1985**, *5*, 123−127.
(56) Yang, P. C.; Pickelman, D. M.; Woo, E. P. *Proc. Int. SAMPE Symp.* **1990**, *35*, 1131.
(57) Yang, P. C.; Woo, E. P.; Laman, S. A.; Jakubowski, J. J.; Pickelman, D. M.; Sue, H. S. *Proc. Int. SAMPE Symp.* **1991**, *36*, 431.
(58) Sachdeva, Y. P. *Int. SAMPE Technol.* **1989**, *21*, 1018.
(59) Moloney, A. C.; Kausch, H. H.; Stieger, H. R. The fracture of particulate-filled epoxide resins. *J. Mater. Sci.* **1983**, *18*, 208−216.
(60) Spanoudakis, J.; Young, R. J. Crack propagation in a glass particle-filled epoxy resin. *J. Mater. Sci.* **1984**, *19*, 473−486.
(61) Hedrick, J. L.; Yilgör, I.; Wilkes, G. L.; McGrath, J. E. Chemical modification of matrix Resin networks with engineering thermoplastics. *Polym. Bull.* **1985**, *13*, 201−208.
(62) Hedrick, J. L.; Yilgor, I.; Jurek, M.; Hedrick, J. C.; Wilkes, G. L.; McGrath, J. E. Chemical Modification of Matrix Resin Networks with Engineering Thermoplastics: 1. Synthesis, Morphology, Physical Behaviour and Toughening Mechanisms of Poly(arylene Ether Sulphone) Modified Epoxy Networks. *Polymer* **1991**, *32*, 2020−2032.
(63) Cecere, J. A.; Mcgrath, J. E.; Hedrick, J. L. Morphology and properties of amine terminated poly (arylene ether ketone) and poly (arylene ether sulfone) modified epoxy resin systems. *NASA Technical Reports Server*, 1986.
(64) Raghava, R. S. Development and Characterization of Thermosetting-thermoplastic Polymer Blends for Applications in Damage-tolerant Composites. *J. Polym. Sci., Part B: Polym. Phys.* **1988**, *26*, 65−81.
(65) Bucknall, C. B.; Gilbert, A. H. Toughening Tetrafunctional Epoxy Resins Using Polyetherimide. *Polymer* **1989**, *30*, 213−217.
(66) Pearson, R. A.; Yee, A. F. The Preparation and Morphology of Ppo Epoxy Blends. *J. Appl. Polym. Sci.* **1993**, *48*, 1051−1060.
(67) Oyanguren, P. A.; Galante, M. J.; Andromaque, K.; Frontini, P. M.; Williams, R. J. J. Development of Bicontinuous Morphologies in Polysulfone − Epoxy Blends. *Polymer* **1999**, *40*, 5249−5255.
(68) Hodgkin, J. H.; Simon, G. P.; Varley, R. J. Thermoplastic Toughening of Epoxy Resins: A Critical Review. *Polym. Adv. Technol.* **1998**, *9*, 3−10.
(69) Kinloch, A. J.; Taylor, A. C. The Toughening of Cyanate-Ester Polymers Part II- Chemical Modification. *J. Mater. Sci.* **2003**, *38*, 65−79.
(70) Marieta, C.; Schulz, E.; Irusta, L.; Gabilondo, N.; Tercjak, A.; Mondragon, I. Evaluation of Fiber Surface Treatment and Toughening of Thermoset Matrix on the Interfacial Behaviour of Carbon Fiber-Reinforced Cyanate Matrix Composites. *Compos. Sci. Technol.* **2005**, *65*, 2189−2197.
(71) Tao, Q.; Wang, M.; Gan, W.; Yu, Y.; Tang, X.; Li, S.; Zhuang, J. Studies on the Phase Separation of Poly(ether Imide)-Modified Cyanate Ester Resin. *J. Macromol. Sci., Part A: Pure Appl.Chem.* **2003**, *40*, 1199−1211.
(72) Hwang, J. W.; Cho, K.; Yoon, T. H.; Park, C. E. Effects of molecular weight of polysulfone on phase separation behavior for cyanate ester/polysulfone blends. *J. Appl. Polym. Sci.* **2000**, *77*, 921−927.
(73) Woo, E. M.; Shimp, D. A.; Seferis, J. C. Phase Structure and Toughening Mechanism of a Thermoplastic-Modified Aryl Dicyanate. *Polymer* **1994**, *35*, 1658−1665.
(74) Mondragón, I.; Solar, L.; Nohales, A.; Vallo, C. I.; Gómez, C. M. Properties and Structure of Cyanate Ester/polysulfone/organoclay Nanocomposites. *Polymer* **2006**, *47*, 3401−3409.
(75) Biron, M. *Thermoplastics and thermoplastic composites*; Elsevier: Amsterdam, 2012.
(76) Wang, M.; Yu, Y.; Zhan, G.; Tang, X.; Li, S. Morphology and Mechanical Properties of Poly(ether-Imide)-Modified Polycyanurates. *Colloid Polym. Sci.* **2006**, *284*, 1379−1385.
(77) Rau, A. V.; Srinivasan, S. A.; McGrath, J. E.; Loos, A. C. Resin Transfer Moulding (RTM) with Toughened Cyanate Ester Resin Systems. *Polym. Compos.* **1998**, *19*, 166−179.
(78) Uhlig, C.; Bauer, M.; Bauer, J.; Kahle, O.; Taylor, A. C.; Kinloch, A. J. Influence of Backbone Structure, Conversion and Phenolic Co-Curing of Cyanate Esters on Side Relaxations, Fracture Toughness, Flammability Properties and Water Uptake and Toughening with Low Molecular Weight Polyethersulphones. *React. Funct. Polym.* **2017**, 1−21.
(79) Marieta, C.; Del Rio, M.; Harismendy, I.; Mondragon, I. Effect of the Cure Temperature on the Morphology of a Cyanate Ester Resin Modified with a Thermoplastic: Characterization by Atomic Force Microscopy. *Eur. Polym. J.* **2000**, *36*, 1445−1454.
(80) Srinivasan, S. A.; McGrath, J. E. Amorphous phenolphthalein-based poly (arylene ether)-modified cyanate ester networks: Effect of thermal cure cycle on morphology and toughenability. *J. Appl. Polym. Sci.* **1997**, *64*, 167−178.
(81) Srinivasan, S. a.; McGrath, J. E. Amorphous Phenolphthalein-Basedpoly(arylene Ether) Modified Cyanate Ester Networks: 1. Effect of Molecular Weight and Backbone Chemistry on Morphology and Toughenability. *Polymer* **1998**, *39*, 2415−2427.
(82) Harvey, B. G.; Guenthner, A. J.; Yandek, G. R.; Cambrea, L. R.; Meylemans, H. A.; Baldwin, L. C.; Reams, J. T. Synthesis and Characterization of a Renewable Cyanate Ester/polycarbonate Network Derived from Eugenol. *Polymer* **2014**, *55*, 5073−5079.
(83) Fainleib, A. M.; Hourston, D. J.; Grigoryeva, O. P.; Shantalii, T. A.; Sergeeva, L. M. Structure Development in Aromatic Polycyanurate Networks Modified with Hydroxyl-Terminated Polyethers. *Polymer* **2001**, *42*, 8361−8372.

DOI: 10.1021/acs.iecr.7b05202
Ind. Eng. Chem. Res. 2018, 57, 4479−4504

(84) Iijima, T.; Kaise, T.; Tomoi, M. Modification of cyanate ester resin by soluble polyimides. *J. Appl. Polym. Sci.* **2003**, *88*, 1−11.
(85) Vijayan P, P.; Puglia, D.; Al-Maadeed, M. A. S.; Kenny, J. M.; Thomas, S. Elastomer/thermoplastic modified epoxy nanocomposites: The hybrid effect of 'micro' and 'nano' scale. *Mater. Sci. Eng., R* **2017**, *116*, 1−29.
(86) Guan, Q.; Yuan, L.; Zhang, Y.; Gu, A.; Liang, G. Improving the mechanical, thermal, dielectric and flame retardancy properties of cyanate ester with the encapsulated epoxy resin-penetrated aligned carbon nanotube bundle. *Composites, Part B* **2017**, *123*, 81−91.
(87) Goertzen, W. K.; Kessler, M. R. Dynamic mechanical analysis of fumed silica/cyanate ester nanocomposites. *Composites, Part A* **2008**, *39*, 761−768.
(88) Goertzen, W. K.; Kessler, M. R. Thermal expansion of fumed silica/cyanate ester nanocomposites. *J. Appl. Polym. Sci.* **2008**, *109*, 647−653.
(89) Badrinarayanan, P.; Rogalski, M. K.; Kessler, M. R. Carbon Fiber-Reinforced Cyanate Ester/nano-ZrW2O8 Composites with Tailored Thermal Expansion. *ACS Appl. Mater. Interfaces* **2012**, *4*, 510−517.
(90) Pan, Y.; Xu, Y.; An, L.; Lu, H.; Yang, Y.; Chen, W.; Nutt, S. Hybrid Network Structure and Mechanical Properties of Rodlike Silicate/cyanate Ester Nanocomposites. *Macromolecules* **2008**, *41*, 9245−9258.
(91) Wooster, T. J.; Abrol, S.; MacFarlane, D. R. Polymeric Toughening of Particle Filled Cyanate Ester Composites. *Macromol. Mater. Eng.* **2005**, *290*, 961−969.
(92) Xie, C.; Li, Y.; Han, Y. Fabrication and properties of CTBN/Si3N4/cyanate ester nanocomposites. *Polym. Compos.* **2016**, *37*, 2522−2526.
(93) Pearson, R. A. Toughening Epoxies Using Rigid Thermoplastic Particles. *Adv. Chem. Ser.* **1993**, *233*, 405−425.
(94) Pearson, R. A.; Yee, A. F. Toughening Mechanisms in Thermoplastic-Modified Epoxies: 1. Modification Using Poly(phenylene Oxide). *Polymer* **1993**, *34*, 3658−3670.
(95) Lange, F. F. The Interaction of a Crack Front with a Second-Phase Dispersion. *Philos. Mag.* **1970**, *22*, 983−992.
(96) Kunz-Douglass, S.; Beaumont, P. W. R.; Ashby, M. F. A Model for the Toughness of Epoxy-Rubber Particulate Composites. *J. Mater. Sci.* **1980**, *15*, 1109−1123.
(97) Kinloch, A. J.; Shaw, S. J.; Hunston, D. L. Deformation and fracture behaviour of a rubber-toughened epoxy: 2. Failure criteria. *Polymer* **1983**, *24*, 1355−1363.
(98) Huang, Y.; Hunston, D. L.; Kinloch, A. J.; Riew, C. K. Mechanisms of toughening thermoset resins. *Adv. Chem. Ser.* **1993**, *233*, 1−35.
(99) Kinloch, A. J.; Maxwell, D.; Young, R. J. Micromechanisms of crack propagation in hybrid-particulate composites. *J. Mater. Sci. Lett.* **1985**, *4*, 1276−1279.
(100) Evans, A. G. The strength of brittle materials containing second phase dispersions. *Philos. Mag.* **1972**, *26*, 1327−1344.
(101) Yee, A. F.; Li, D.; Li, X. The importance of constraint relief caused by rubber cavitation in the toughening of epoxy. *J. Mater. Sci.* **1993**, *28*, 6392−6398.
(102) Faber, K. T.; Evans, A. G. Crack Deflection Processes-I. Theory. *Acta Metall.* **1983**, *31*, 565−576.
(103) Kinloch, A. J.; Yuen, M. L.; Jenkins, S. D. Thermoplastic-Toughened Epoxy Polymers. *J. Mater. Sci.* **1994**, *29*, 3781−3790.
(104) Dompas, D.; Groeninckx, G. Toughening Behaviour of Rubber-Modified Thermoplastic Polymers Involving Very Small Rubber Particles: 1. A Criterion for Internal Rubber Cavitation. *Polymer* **1994**, *35*, 4743−4749.
(105) Pearson, R. A.; Yee, A. F. Toughening mechanisms in elastomer-modified epoxies. *J. Mater. Sci.* **1989**, *24*, 2571−2580.
(106) Gazit, S.; Bell, J. P. Impact performance of epoxy resins with poly(n-butyl acrylate) as the reactive liquid rubber modifier. *ACS Symp. Ser.* **1983**, *221*, 69−83.
(107) Muratoglu, O. K.; Argon, A. S.; Cohen, R. E.; Weinberg, M. Toughening mechanism of rubber-modified polyamides. *Polymer* **1995**, *36*, 921−930.
(108) McGrail, P. T.; Jenkins, S. D. Some Aspects of Interlaminar Toughening: Reactively Terminated Thermoplastic Particles in Thermoset Composites. *Polymer* **1993**, *34*, 677−683.
(109) Kim, Y. S.; Min, H. S.; Kim, S. C. Polyetherimide/dicyanate Semi-Interpenetrating Polymer Networks Having Morphology Spectrum. *Macromol. Res.* **2002**, *10*, 60−66.
(110) Brown, R. *Handbook of polymer testing: physical methods*; CRC Press: Boca Raton, FL, 1999.
(111) Mondragon, I.; Solar, L.; Nohales, A.; Vallo, C. I.; Gomez, C. M. Properties and structure of cyanate ester/polysulfone/organoclay nanocomposites. *Polymer* **2006**, *47*, 3401−3409.
(112) Cardwell, B. J.; Yee, A. F. Toughening of epoxies through thermoplastic crack bridging. *J. Mater. Sci.* **1998**, *33*, 5473−5484.
(113) Rutnakornpituk, M. Thermoplastic toughened epoxy networks and their toughening mechanisms in some systems. *NUJST* **2005**, *13*, 73−83.
(114) Yoon, T. H.; Priddy, D. B.; Lyle, G. D.; McGrath, J. E. Mechanical and morphological investigations of reactive polysulfone toughened epoxy networks. *Macromol. Symp.* **1995**, *98*, 673−686.
(115) Brooker, R. D.; Kinloch, A. J.; Taylor, A. C. The morphology and fracture properties of thermoplastic-toughened epoxy polymers. *J. Adhes.* **2010**, *86*, 726−741.
(116) Shah, V. *Handbook of plastics testing and failure analysis*; John Wiley & Sons: New York, 2007; p *21*.
(117) Cheremisinoff, N. P. *Polymer characterization: laboratory techniques and analysis*; Noyes Publications: Westwood, NJ, 1996.
(118) Suman, J. N.; Kathi, J.; Tammishetti, S. Thermoplastic modification of monomeric and partially polymerized Bisphenol A dicyanate ester. *Eur. Polym. J.* **2005**, *41*, 2963−2972.
(119) Shimp, D. A. (Hi-Tek Polymers Inc.). Metal acetylacetonate/alkylphenol curing catalyst for polycyanate esters of polyhydric phenols. U.S. Patent 4,847,233, 1989.
(120) Shimp, D. A. (Interez Inc.). Metal acetylacetonate/alkylphenol curing catalyst for polycyanate esters of polyhydric phenols. U.S. Patent 4,785,075, 1988.
(121) Osei-Owusu, A.; Martin, G. C.; Gotro, J. T. Analysis of the curing behavior of cyanate ester resin systems. *Polym. Eng. Sci.* **1991**, *31*, 1604−1609.
(122) Parlevliet, P. P.; Meier, C.; Metzner, C. Composite Manufacturing Technologies for Novel High Temperature Composites. *Eur. Conf. Compos. Mater.* **2016**, 26−30.
(123) Hillermeier, R. W.; Hayes, B. S.; Seferis, J. C. Processing of Highly Elastomeric Toughened Cyanate Esters through a Modified Resin Transfer Molding Technique. *Polym. Compos.* **1999**, *20*, 155−165.
(124) Wang, Y. S.; Wu, Y. J. (Hexcel Corp.). Thermoplastic-toughened cyanate ester resin composites with low heat release properties. U.S. Patent 8,283,408, 2012.
(125) Nair, C. R.; Mathew, D.; Ninan, K. N. Cyanate ester resins, recent developments. *New Polymerization Techniques and Synthetic Methodologies*; Springer: Berlin/Heidelberg, 2001; 1−99.
(126) Esslinger, J. R.; Fruchtnicht, O. C. Cyanate ester matrix technology for improved thermal performance of filament wound missile structures. *SAMPE J.* **2004**, *40*, 9−15.
(127) Tian, J.; Zhang, S.; Jiang, X.; Hou, C.; Ma, G. Research on Application of Modified Cyanate Ester on Filament Winding. *Fiber Composites* **2008**, *3*, 011.
(128) Cui, Y. Q.; Yin, Z. W. Carbon-fibre-reinforced modified cyanate ester winding composites and their thermomechanical properties. *High Perform. Polym.* **2018**, 095400831775352.
(129) Hamerton, I.; Barton, J. M.; Chaplin, A.; Howlin, B. J.; Shaw, S. J. The development of novel functionalised aryl cyanate esters. Part 2. Mechanical properties of the polymers and composites. *Polymer* **2001**, *42*, 2307−2319.

DOI: 10.1021/acs.iecr.7b05202
Ind. Eng. Chem. Res. 2018, 57, 4479−4504

(130) Hayes, B. S.; Seferis, J. C.; Parker, G. A. Rubber modification of low temperature cure cyanate ester matrices and the performance in glass fabric composites. *Polym. Eng. Sci.* **2000**, *40*, 1344−1349.
(131) Shivakumar, K. N.; Chen, H.; Holloway, G. Effect of thermal fatigue on tensile and flexural properties of carbon/cyanate ester pultruded composite. *J. Reinf. Plast. Compos.* **2009**, *28*, 675−689.
(132) Shivakumar, K.; Chen, H.; Holloway, G. Gas turbine environment effect on morphology and mechanical properties of pultruded composite. *J. Appl. Polym. Sci.* **2008**, *108*, 189−198.
(133) Laurenzi, S.; Marchetti, M. Advanced Composite Materials by Resin Transfer Molding for Aerospace Applications. *Composites and Their Properties*; InTech, 2012; pp 197−226.
(134) Hillermeier, R. W.; Seferis, J. C. Environmental Effects on Thermoplastic and Elastomer Toughened Cyanate Ester Composite Systems. *J. Appl. Polym. Sci.* **2000**, *77*, 556−567.
(135) Angell, R. G., Jr.; Michno, M. J., Jr.; Konrad, J. M.; Hobbs, K. E. (BP Corporation North America Inc.). Hot-melt prepreg tow process. U.S. Patent 4,804,509, 1989.
(136) Qi, B.; Raju, J.; Kruckenberg, T.; Stanning, R. A Resin Film Infusion Process for Manufacture of Advanced Composite Structures. *Compos. Struct.* **1999**, *47*, 471−476.
(137) Letterman, L. E. (Boeing Co.). Resin film infusion process and apparatus. U.S. Patent 4,622,091, 1986.
(138) Starr, T. F.; Ketel, J. A. *Composites and pultrusion. Pultrusion for engineers*; Woodhead Publishing Limited: Cambridge, 2000; pp 1−18.
(139) Shaw-Stewart, D.; Sumerak, J. E. *The Pultrusion Process*. Woodhead Publishing Limited, 2000.
(140) Jayaraman, K.; Kotaki, M.; Zhang, Y.; Mo, X.; Ramakrishna, S. Recent advances in polymer nanofibers. *J. Nanosci. Nanotechnol.* **2004**, *4*, 52−65.
(141) Beckermann, G. W.; Pickering, K. L. Mode I and Mode II Interlaminar Fracture Toughness of Composite Laminates Interleaved with Electrospun Nanofibre Veils. *Composites, Part A* **2015**, *72*, 11−21.
(142) Huang, Z. M.; Zhang, Y. Z.; Kotaki, M.; Ramakrishna, S. A review on polymer nanofibers by electrospinning and their applications in nanocomposites. *Compos. Sci. Technol.* **2003**, *63*, 2223−2253.
(143) Wu, X. F.; Yarin, A. L. Recent progress in interfacial toughening and damage self-healing of polymer composites based on electrospun and solution-blown nanofibers: An overview. *J. Appl. Polym. Sci.* **2013**, *130*, 2225−2237.
(144) Kim, J. S.; Reneker, D. H. Mechanical properties of composites using ultrafine electrospun fibers. *Polym. Compos.* **1999**, *20*, 124−131.
(145) van der Heijden, S.; Daelemans, L.; De Schoenmaker, B.; De Baere, I.; Rahier, H.; Van Paepegem, W.; De Clerck, K. Interlaminar toughening of resin transfer moulded glass fibre epoxy laminates by polycaprolactone electrospun nanofibres. *Compos. Sci. Technol.* **2014**, *104*, 66−73.
(146) Li, G.; Li, P.; Yu, Y.; Jia, X.; Zhang, S.; Yang, X.; Ryu, S. Novel Carbon Fiber/epoxy Composite Toughened by Electrospun Polysulfone Nanofibers. *Mater. Lett.* **2008**, *62*, 511−514.
(147) Anand, A.; Kumar, N.; Harshe, R.; Joshi, M. Glass/epoxy structural composites with interleaved nylon 6/6 nanofibers. *J. Compos. Mater.* **2017**, *51*, 3291−3298.
(148) Zhang, J.; Lin, T.; Wang, X. Electrospun Nanofibre Toughened Carbon/epoxy Composites: Effects of Polyetherketone Cardo (PEK-C) Nanofibre Diameter and Interlayer Thickness. *Compos. Sci. Technol.* **2010**, *70*, 1660−1666.
(149) Zhou, F. L.; Gong, R. H.; Porat, I. Mass Production of Nanofibre Assemblies: By Electrostatic Spinning. *Polym. Int.* **2009**, *58* (4), 331−342.
(150) Badrossamay, M. R.; McIlwee, H. A.; Goss, J. A.; Parker, K. K. Nanofiber assembly by rotary jet-spinning. *Nano Lett.* **2010**, *10*, 2257−2261.
(151) Weitz, R. T.; Harnau, L.; Rauschenbach, S.; Burghard, M.; Kern, K. Polymer nanofibers via nozzle-free centrifugal spinning. *Nano Lett.* **2008**, *8*, 1187−1191.
(152) Mahalingam, S.; Ren, G. G.; Edirisinghe, M. J. Rheology and pressurised gyration of starch and starch-loaded poly (ethylene oxide). *Carbohydr. Polym.* **2014**, *114*, 279−287.
(153) Mahalingam, S.; Raimi-Abraham, B. T.; Craig, D. Q.; Edirisinghe, M. Formation of protein and protein−gold nanoparticle stabilized microbubbles by pressurized gyration. *Langmuir* **2015**, *31*, 659−666.
(154) Hammami, M. A.; Krifa, M.; Harzallah, O. Centrifugal force spinning of PA6 nanofibers−processability and morphology of solution-spun fibers. *J. Text. Inst.* **2014**, *105*, 637−647.
(155) Hong, X.; Mahalingam, S.; Edirisinghe, M. Simultaneous Application of Pressure-Infusion-Gyration to Generate Polymeric Nanofibers. *Macromol. Mater. Eng.* **2017**, *302*, 1−16.
(156) Lau, K. S. High-performance polyimides and high temperature resistant polymers. *Handbook of Thermoset Plastics*, 3rd ed.; William Andrew, 2014; pp 297−424, DOI: 10.1016/B978-1-4557-3107-7.00010-5.
(157) Hamerton, I.; Mooring, L. The Use of Thermosets in Aerospace Applications. *Thermosets Struct. Prop. Appl.* **2012**, 189−227.
(158) Kandelbauer, A. *Handbook of Thermoset Plastics: 11. Cyanate Esters*; Elsevier: Amsterdam, 2013.
(159) Ganguli, S.; Dean, D.; Jordan, K.; Price, G.; Vaia, R. Mechanical properties of intercalated cyanate ester−layered silicate nanocomposites. *Polymer* **2003**, *44*, 1315−1319.
(160) Fabian, P. E.; Munshi, N. A.; Denis, R. J. Radiation-resistant vacuum impregnation resin systems for fusion magnet insulation. *AIP Conf. Proc.* **2002**, 614.
(161) Prokopec, R.; Humer, K.; Maix, R. K.; Fillunger, H.; Weber, H. W. Characterization of advanced cyanate ester/epoxy insulation systems before and after reactor irradiation. *Fusion Eng. Des.* **2010**, *85*, 227−233.
(162) Balde, J.; Messner, G. Low Dielectric Constant—The Substrate of the Future. *Circuit World* **1987**, *14*, 11−14.
(163) Fujimoto, D.; Mizuno, Y.; Takano, N.; Sase, S.; Negishi, H.; Sugimura, T. Low-transmission-loss modified cyanate ester materials for high-frequency applications. *Polymers Adhesives in Microelectronics Photonics* **2002**, 114−119.
(164) Paulus, J. R. High performance laminate systems for high speed electronics Applications. *Circuit World* **1989**, *15*, 19−24.
(165) Deutsch, A.; Surovic, C. W.; Lanzetta, A. P.; Ainspan, H. A.; Abbiate, J. C.; Viehbeck, A.; Hedrick, J. C.; Shaw, J. M.; Tisdale, S. L.; Foster, E. F.; Coteus, P. W. Broadband characterization of low dielectric constant and low dielectric loss CYTUF cyanate ester printed circuit board material. *IEEE Trans. Compon., Packag., Manuf. Technol., Part B* **1996**, *19*, 331−337.

DOI: 10.1021/acs.iecr.7b05202
Ind. Eng. Chem. Res. 2018, 57, 4479−4504